Appendix D

Marine Mammal Modeling

TABLE OF CONTENTS

LIST OF FIGURES

LIST OF TABLES

This page intentionally left blank

D MARINE MAMMAL MODELING

D.1 BACKGROUND AND OVERVIEW

All marine mammals are protected under the Marine Mammal Protection Act (MMPA). The MMPA prohibits, with certain exceptions, the unauthorized take of marine mammals in U.S. waters and by U.S. citizens on the high seas, and the importation of marine mammals and marine mammal products into the U.S.

The Endangered Species Act of 1973 (ESA) provides for the conservation of species that are endangered or threatened throughout all or a significant portion of their range, and the conservation of their ecosystems. A "species" is considered endangered if it is in danger of extinction throughout all or a significant portion of its range. A species is considered threatened if it is likely to become an endangered species within the foreseeable future. There are marine mammals, already protected under MMPA, listed as either endangered or threatened under ESA, and afforded special protections.

Actions involving sound in the water include the potential to harass marine animals in the surrounding waters. Demonstration of compliance with MMPA and the ESA, using best available science, has been assessed using criteria and thresholds accepted or negotiated, and described here.

Sections of the MMPA (16 United States Code [U.S.C.] 1361 et seq.) direct the Secretary of Commerce to allow, upon request, the incidental, but not intentional, taking of small numbers of marine mammals by U.S. citizens who engage in a specified activity, other than commercial fishing, within a specified geographical region.

Authorization for incidental takings may be granted if the National Marine Fisheries Service (NMFS) finds that the taking will have no more than a negligible impact on the species or stock(s), will not have an immitigable adverse impact on the availability of the species or stock(s) for subsistence uses, and that the permissible methods of taking, and requirements pertaining to the mitigation, monitoring and reporting of such taking are set forth.

NMFS has defined negligible impact in 50 Code of Federal Regulations (CFR) 216.103 as an impact resulting from the specified activity that cannot be reasonably expected to, and is not reasonably likely to, adversely affect the species or stock through effects on annual rates of recruitment or survival.

Subsection 101(a)(5)(D) of the MMPA established an expedited process by which citizens of the United States can apply for an authorization to incidentally take small numbers of marine mammals by harassment. The National Defense Authorization Act of 2004 (NDAA) (Public Law 108-136) removed the small numbers limitation and amended the definition of "harassment" as it applies to a military readiness activity to read as follows:

> (i) *any act that injures or has the significant potential to injure a marine mammal or marine mammal stock in the wild [Level A Harassment]; or*
>
> (ii) *any act that disturbs or is likely to disturb a marine mammal or marine mammal stock in the wild by causing disruption of natural behavioral patterns, including, but not limited to, migration, surfacing, nursing, breeding, feeding, or sheltering, to a point where such behavioral patterns are abandoned or significantly altered [Level B Harassment].*

The primary potential impact to marine mammals from underwater acoustics is Level B harassment from exposure to various sources of sound in the water including sonar and explosives. The criteria for modeling impacts from these sources are detailed in the following sections.

D.1.1 Acoustic Sound Sources

The amount of Threshold Shift depends on the amplitude, duration, frequency, and temporal pattern of the sound exposure. Threshold shifts will generally increase with the amplitude and duration of sound exposure. For continuous sounds, exposures of equal energy will lead to approximately equal effects (Ward 1997). For intermittent sounds, less Threshold Shift will occur than from a continuous exposure with the same energy (some recovery will occur between exposures) (Kryter et al., 1966; Ward 1997). The magnitude of Threshold Shift normally decreases with the amount of time post-exposure (Miller 1974).

Permanent Threshold Shift (PTS) is non-recoverable and results from the destruction of tissues within the auditory system. PTS therefore qualifies as an injury and is classified as Level A harassment under the MMPA. The smallest amount of PTS (onset- PTS) is taken to be the indicator for the smallest degree of injury that can be measured. The acoustic exposure associated with onset-PTS is used to define the outer limit of the Level A exposure zone.

If the TS eventually returns to zero (the threshold returns to the pre-exposure value), the TS is a Temporary Threshold Shift (TTS). TTS is, from recent rulings (NOAA 2001; 2002a), considered to result from the temporary, non-injurious distortion of hearing-related tissues. The smallest measurable amount of TTS (onset-TTS) is taken as the best indicator for slight temporary sensory impairment. Because it is considered non-injurious, the acoustic exposure associated with onset-TTS is used to define the outer limit of the portion of the Level B exposure zone attributable to physiological effects. This follows from the concept that hearing loss potentially affects an animal's ability to react normally to the sounds around it. Therefore, the potential for TTS is considered as Level B harassment caused by physiological effects on the auditory system.

The exposure threshold established for onset-TTS is 195 dB re 1μPa^2-s. This result is supported by the short-duration tone data of Finneran et al. (2002, 2005) and the long-duration sound data from Nachtigall et al., (2003). Together, these data demonstrate that TTS in small odontocetes is correlated with the received EL and that onset-TTS exposures are fit well by an equal-energy line passing through 195 dB re 1μPa^2-s. Absent any additional data for other species and being that it is likely that small odontocetes are more sensitive to the mid-frequency active/high-frequency active frequency levels of concern, this threshold is used for analysis for all cetacea.

The PTS thresholds established for use in this analysis are based on a 20 dB increase in exposure EL over that required for onset-TTS. The 20 dB value is based on estimates from terrestrial mammal data of PTS occurring at 40 dB or more of TS, and on TS growth occurring at a rate of 1.6 dB/dB increase in exposure EL. This is conservative because: (1) 40 dB of TS is actually an upper limit for TTS used to approximate onset-PTS, and (2) the 1.6 dB/dB growth rate is the highest observed in the data from Ward et al. (1958, 1959). Using this estimation method (20 dB increase from onset-TTS) for analysis, the PTS threshold for cetacea is 215 dB re 1μPa^2-s.

Unlike cetaceans, the TTS and PTS thresholds used for pinnipeds vary with species. Otariids have thresholds of 206 dB re 1μPa^2-s for TTS and 226 dB re 1μPa^2-s for PTS. Northern elephant seals are similar to otariids (TTS = 204 dB re 1μPa^2-s, PTS = 224 dB re 1μPa^2-s) but are lower for harbor seals (TTS = 183 dB re 1μPa^2-s, PTS = 203 dB re 1μPa^2-s). A certain proportion of marine mammals is expected to experience behavioral disturbance at different received sound pressure levels and are counted as Level B harassment takes. The details of this theory and calculation are described in the Risk Function section. Table D-1 summarizes the threshold levels for analysis of non-explosive sound sources used during Navy training activities in the Gulf of Alaska (GOA) Temporary Maritime Activities Area (TMAA).

Table D-1 - Non-Explosive Sound Source Threshold Levels

Physiological Effects			
Animal	**Criteria**	**Threshold (re 1μPa^2-s)**	**MMPA Effect**
Cetacean	TTS PTS	195 215	Level B Harassment Level A Harassment
Pinnipeds			
Northern Elephant Seal	TTS PTS	204 224	Level B Harassment Level A Harassment
Steller Sea Lion	TTS PTS	206 226	Level B Harassment Level A Harassment
Northern Fur Seal	TTS PTS	206 226	Level B Harassment Level A Harassment

D.1.2 Explosives

For underwater explosions resulting from use of live ordnance in the TMAA, in the absence of any mitigation or monitoring measures, there is a very small chance that a marine mammal could be injured or killed when exposed to the energy generated from an explosive force. Analysis of sound and pressure impacts from underwater explosions is based on criteria and thresholds initially presented in U.S. Navy Environmental Impact Statements for ship shock trials of the Seawolf submarine and the Winston Churchill (DDG 81), and subsequently adopted by NMFS.

Non-lethal injurious impacts (Level A Harassment) are defined in those documents as tympanic membrane (TM) rupture and the onset of slight lung injury. The threshold for Level A Harassment corresponds to a 50-percent rate of TM rupture, which can be stated in terms of an energy flux density (EFD) value of 205 dB re 1μPa^2-s. TM rupture is well-correlated with permanent hearing impairment. Ketten (1998) indicates a 30-percent incidence of permanent threshold shift (PTS) at the same threshold.

The criteria for onset of slight lung injury were established using partial impulse because the impulse of an underwater blast wave was the parameter that governed damage during a study using mammals, not peak pressure or energy (Yelverton, 1981). Goertner (1982) determined a way to calculate impulse values for injury at greater depths, known as the Goertner "modified" impulse pressure. Those values are valid only near the surface because as hydrostatic pressure increases with depth, organs like the lung, filled with air, compress. Therefore the "modified" impulse pressure thresholds vary from the shallow depth starting point as a function of depth.

The shallow depth starting points for calculation of the "modified" impulse pressures are mass-dependent values derived from empirical data for underwater blast injury (Yelverton, 1981). During the calculations, the lowest impulse and body mass for which slight, and then extensive, lung injury found during a previous study (Yelverton et al, 1973) were used to determine the positive impulse that may cause lung injury. The Goertner model is sensitive to mammal weight such that smaller masses have lower thresholds for positive impulse so injury and harassment will be predicted at greater distances from the source for them. Impulse thresholds of 13.0 and 31.0 psi-msec, found to cause slight and extensive injury in a dolphin calf, were used as thresholds in the analysis contained in this document.

Level B (behavior response) Harassment includes temporary (auditory) threshold shift (TTS), a slight, recoverable loss of hearing sensitivity. One criterion used for TTS, the total energy flux density of the sound, is a threshold of 182 dB re 1µPa^2-s maximum EFD level in any 1/3-octave band above 100 Hz for toothed whales (e.g., dolphins). A second criterion, a maximum allowable peak pressure of 23 psi, has recently been established by NMFS to provide a more conservative range for TTS when the explosive or animal approaches the sea surface, in which case explosive energy is reduced, but the peak pressure is not. NMFS applies the more conservative of these two.

For multiple successive explosions (MSE) occurring underwater, the acoustic criterion for non-TTS behavioral disturbance is used to account for behavioral effects significant enough to be judged as harassment, but occurring at lower sound energy levels than those that may cause TTS. The non-TTS threshold is derived following the approach of the Churchill Final Environmental Impact Statement (FEIS) for the energy-based TTS threshold. The research on pure-tone exposures reported in Schlundt et al. (2000) and Finneran and Schlundt (2004) provided a threshold of 192 dB re 1µPa^2-s as the lowest TTS value. This value for pure-tone exposures is modified for explosives by (a) interpreting it as an energy metric, (b) reducing it by 10 dB to account for the time constant of the mammal ear, and (c) measuring the energy in 1/3 octave bands, the natural filter band of the ear. The resulting TTS threshold for explosives is 182 dB re 1µPa^2-s in any 1/3 octave band. As reported by Schlundt et al. (2000) and Finneran and Schlundt (2004), instances of altered behavior in the pure-tone research generally began five dB lower than those causing TTS. The non-TTS threshold is therefore derived by subtracting 5 dB from the 182 dB re 1µPa^2-s in any 1/3 octave band threshold, resulting in a 177 dB re 1µPa^2-s (EL) sub-TTS behavioral disturbance threshold for MSE. Table D-2 summarizes the threshold levels for analysis of explosives used in the GOA.

Table D-2 - Explosives Threshold Levels

Threshold Type	Threshold Level
Level A – 50% Eardrum rupture	205 dB re 1µPa^2-s
Temporary Threshold Shift (TTS) (peak 1/3 octave energy)	182 dB re 1µPa^2-s
Sub-TTS Threshold for Multiple Successive Explosions (peak 1/3 octave energy)	177 dB re 1µPa^2-s
Temporary Threshold Shift (TTS) (peak pressure)	23 psi
Level A – Slight lung injury (positive impulse)	13 psi-ms
Fatality – 1% Mortal lung injury (positive impulse)	31 psi-ms

The sound sources will be located in an area that is inhabited by species listed as threatened or endangered under the ESA (16 USC §§ 1531-1543). Operation of the sound sources, that is, transmission of acoustic signals in the water column, could potentially cause harm or harassment to listed species.

"Harm" defined under ESA regulations is "…an act which actually kills or injures…" (50 CFR 222.102) listed species. "Harassment" is an "intentional or negligent act or omission which creates the likelihood of injury to wildlife by annoying it to such an extent as to significantly disrupt normal behavioral patterns which include, but are not limited to, breeding, feeding, or sheltering" (50 CFR 17.3).

If a federal agency determines that its proposed action "may affect" a listed species, it is required to consult, either formally or informally, with the appropriate regulator. There is no permit issuance under ESA, rather consultation among the cognizant federal agencies under Section 7 of the ESA. Such consultations would likely be concluded favorably, subject to requirements that the activity will not appreciably reduce the likelihood of the species' survival and recovery and impacts are minimized and mitigated.

D.2 ACOUSTIC SOURCES

The acoustic sources employed in the TMAA are categorized as either broadband (producing sound over a wide frequency band) or narrowband (producing sound over a frequency band that that is small in comparison to the center frequency). In general, the majority of acoustic energy results from narrowband sonars utilized for Anti-Submarine Warfare (ASW) activities and underwater explosions as broadband sources. This delineation of source types has a couple of implications. First, the transmission loss used to determine the impact ranges of narrowband ASW sonars can be adequately characterized by model estimates at a single frequency. Broadband explosives, on the other hand, produce significant acoustic energy across several frequency decades of bandwidth. Propagation loss is sufficiently sensitive to frequency as to require model estimates at several frequencies over such a wide band.

Second, the types of sources have different sets of harassment metrics and thresholds. Energy metrics are defined for both types. However, explosives are impulsive sources that produce a shock wave that dictates additional pressure-related metrics (peak pressure and positive impulse). Detailed descriptions of both types of sources are provided in the following subsections.

D.2.1 Acoustic Sources

Operations in the TMAA involve four (4) types of narrowband sonars, as shown in Table D-3. Harassment estimates are calculated for each source according to the manner in which it operates. For example, the SQS-53 is a hull-mounted, surface ship sonar that operates for many hours at a time, so it is useful to calculate and report SQS-53 harassments per hour of operation. The AQS-22 is a helicopter-deployed sonar, which is lowered into the water, pings a number of times, and then moves to a new location. For the AQS-22, it is useful to calculate and report harassments per dip. The SSQ-62 sonobuoy is modeled at a single depth pinging for a fixed duration, so harassments are accordingly reported per sonobuoy deployed. The following table presents the deploying platform, frequency class, and the reporting metric for each acoustic source analyzed for use in the TMAA.

Table D-3 - Acoustic Sources Analyzed for use in the TMAA

Sonar	Description	Frequency Class	Harassments Reported
SQS-53	Surface ship sonar	Mid-frequency	Per hour
SSQ-62	Sonobuoy sonar	Mid-frequency	Per sonobuoy
AQS-22	Helicopter-dipping sonar	Mid-frequency	Per dip
SQS-56	Surface ship sonar	Mid-frequency	Per hour
MK-84 Range Pingers	Surface pingers	High-frequency	Per day
PUTR Transponders	Bottom pingers	Mid-frequency	Per day
MK-39 EMATT	Training target	Low frequency	Per hour
BQQ-10	Submarine sonar	Classified	Per hour
BQS-15	Submarine sonar	Classified	Per hour
SUS, MK-84	Expendable buoy	Mid-frequency	Per hour

The acoustic modeling that is necessary to support the harassment estimates for each of these sonars relies upon a generalized description of the manner of the sonar's operating modes. This description includes the following:

- "Effective" energy source level—This is the level relative to $1\mu Pa^2$-s of the integral over frequency and time of the square of the pressure and is given by the total energy level across the band of the source, scaled by the pulse length ($10 \log_{10}$ [pulse length]).

- Source depth—Depth of the source in meters.
- Nominal frequency - Typically the center band of the source emission. These are frequencies that have been reported in open literature and are used to avoid classification issues. Differences between these nominal values and actual source frequencies are small enough to be of little consequence to the output impact volumes.
- Source directivity - The source beam is modeled as the product of a horizontal beam pattern and a vertical beam pattern. Two parameters define the horizontal beam pattern:
  - Horizontal beam width—Width of the source beam (degrees) in the horizontal plane (assumed constant for all horizontal steer directions).
  - Horizontal steer direction—Direction in the horizontal in which the beam is steered relative to the direction in which the platform is heading.

  The horizontal beam is assumed to have constant level across the width of the beam with flat, 20-dB down side lobes at all other angles.

  Similarly, two parameters define the vertical beam pattern:

  - Vertical beam width - Width of the source beam (degrees) in the vertical plane measured at the 3-dB down point (assumed constant for all vertical steer directions).
  - Vertical steer direction - Direction in the vertical plane that the beam is steered relative to the horizontal (upward looking angles are positive).

  To avoid sharp transitions that a rectangular beam might introduce, the power response at vertical angle θ is

  $$\text{Power} = \max \{ \sin^2 [n(\theta_s - \theta)] / [n \sin (\theta_s - \theta)]^2,\ 0.01 \},$$

  where θ_s is the vertical beam steer direction, and $n = 2*L/\lambda$ (L = array length, λ = wavelength).

  The beamwidth of a line source is determined by n (the length of the array in half-wavelengths) as $\theta_w = 180^o/n$.

- Ping spacing - Distance between pings. For most sources this is generally just the product of the speed of advance of the platform and the repetition rate of the sonar. Animal motion is generally of no consequence as long as the source motion is greater than the speed of the animal (nominally, 3 knots). For stationary (or nearly stationary) sources, the “average” speed of the animal is used in place of the platform speed. The attendant assumption is that the animals are all moving in the same constant direction.

These parameters are defined for each of the active sound sources in Table D-4 and D-5.

Table D-4 – Source Description of Active Sources used in the TMAA

Sonar	Source Depth	Center Freq	Source Level	Emission Spacing	Vertical Directivity	Horizontal Directivity
SQS-53C	7 m	3.5 kHz	235 dB	154 m	Omni	240^{o} Forward-looking
SSQ-62	27 m	8 kHz	201 dB	450 m	Omni	Omni
AQS-22	27 m	4.1 kHz	217 dB	15 m	Omni	Omni
SQS-56	7 m	7.5 kHz	225 dB	129 m	Omni	90^{o} Forward-looking
MK-84 Range Pingers	7m, 100m	12.9 kHz	194 dB		90 Down	Omni
PUTR Transponders	1,800 m	8.8 kHz	186 dB	Variable	180 Upward	Omni
MK-39 EMATT	100 m	900 Hz	130 dB	Continuous	Omni	Omni
BQQ-10	100 m	Classified	Classified	Classified	Classified	Classified
BQS-15	50 m	Classified	Classified	Classified	Classified	Classified
SUS, MK-84	50 m	3.4 kHz	160 dB	Continuous	Omni	Omni

The following are the usage units for sonar sources in the TMAA (all modeled during the summer season):

Table D-5 – Sonar Usage Units

Sonar	2CSG	1CSG
SQS-53C	578 Hours	289 hours
SSQ-62	267 buoys	133 buoys
AQS-22	192 dips	96 dips
SQS-56	52 hours	26 hours
BQQ-10	48 hours	24 hours
BQS-15	24 hours	12 hours

D.2.2 Explosives

Explosives detonated underwater introduce loud, impulsive, broadband sounds into the marine environment. Three source parameters influence the effect of an explosive: the weight of the explosive material, the type of explosive material, and the detonation depth. The net explosive weight (or NEW) accounts for the first two parameters. The NEW of an explosive is the weight of TNT required to produce an equivalent explosive power.

The detonation depth of an explosive is particularly important due to a propagation effect known as surface-image interference. For sources located near the sea surface, a distinct interference pattern arises from the coherent sum of the two paths that differ only by a single reflection from the pressure-release surface. As the source depth and/or the source frequency decreases, these two paths increasingly, destructively interfere with each other, reaching total cancellation at the surface (barring surface-reflection scattering loss).

For the TMAA, explosive sources having detonations in the water include the following: SSQ-110 EER sonobuoys and MK-82, MK-83, MK-84, BDU-45 bombs, 5” rounds and 76 mm gunnery rounds, MK-48 torpedo, and Maverick missile. The SSQ-110 source can be detonated at several depths within the water column. For this analysis, a relatively shallow depth of 65 ft (20 m) is used to optimize the likelihood of the source being positioned in a surface duct. A source depth of two meters is used for bombs and missiles that do not strike their target. The MK-48 torpedo detonates immediately below the target's hull and a nominal depth of 50 ft (14 m) is used as its source depth in this analysis. For the gunnery rounds, a source depth of one foot is used. The NEW modeled for these sources are as follows:

- SSQ-110 Sonobuoy - 5 pounds
- MK-82 bomb - 238 pounds
- MK-83 bomb - 238 pounds
- MK-83 bomb – 574 pounds
- MK-84 bomb – 945 pounds
- 5" rounds – 9.54 pounds
- 76 mm rounds – 1.6 pounds
- MK-48 torpedo – 851 pounds
- Air-to-Ground (AGM)-65 Maverick Missile – 78.5 pounds

The harassments expected to result from these sources are computed on a per in-water explosive basis. The cumulative effect of a series of explosives can often be derived by simple addition if the detonations are spaced widely in time or space, allowing for sufficient animal movements as to ensure a different population of animals is considered for each detonation.

The cases in which simple addition of the harassment estimates may not be appropriate are addressed by the modeling of a "representative" sinking exercise (SINKEX). In a SINKEX, a decommissioned vessel is towed to a specified deep-water location and there used as a target for a variety of weapons. Although no two SINKEXs are ever the same, a representative case derived from past exercises is described in the Programmatic SINKEX Overseas Environmental Assessment (March 2006) for the Western North Atlantic. Unguided weapons are more frequently off-target and are modeled according to the statistical hit/miss ratios. Note that these hit/miss ratios are artificially low in order to demonstrate a worst-case scenario; they should not be taken as indicative of weapon or platform reliability. With one exception, it is assumed that all missiles in a SINKEX will strike the target vessel. The Maverick missile and bombs used in SINKEX were modeled as missing the target vessel approximately 33 percent of the time. For all live rounds fired in a GUNEX and an estimated 32 percent of rounds fired in SINKEX may explode in the water.

In a SINKEX, weapons are typically fired in order of decreasing range from the source with weapons fired until the target is sunk. A torpedo is used after all munitions have been expended if the target is still afloat. Since the target may sink at any time during the exercise, the actual number of weapons used can vary widely. In the representative case, however, all of the ordnances are assumed expended; this represents the worst case with maximum exposure.

The sequence of weapons firing for the representative SINKEX is described in Table D-6. Guided weapons are nearly 100% accurate and are modeled as hitting the target (that is, no underwater acoustic effect) in all but two cases: (1) the Maverick is modeled as a miss to represent the occasional miss, and (2) the MK-48 torpedo intentionally detonates in the water column immediately below the hull of the target. Unguided weapons are more frequently off-target and are modeled according to the statistical hit/miss ratios. Note that these hit/miss ratios are artificially low in order to demonstrate a worst-case scenario; they should not be taken as indicative of weapon or platform reliability.

Table D-6 – Representative SINKEX Weapons Firing Sequence

Time (Local)	Event Description
0900	Range Control Officer receives reports that the exercise area is clear of non-participant ship traffic, marine mammals, and sea turtles.
0909	Hellfire missile fired, hits target.
0915	2 HARM missiles fired, both hit target (5 minutes apart).
0930	1 Penguin missile fired, hits target.
0940	3 Maverick missiles fired, 2 hit target, 1 misses (5 minutes apart).
1145	1 SM-1 fired, hits target.
1147	1 SM-2 fired, hits target.
1205	5 Harpoon missiles fired, all hit target (1 minute apart).
1300-1335	7 live and 3 inert MK 82 bombs dropped – 7 hit target, 2 live and 1 inert miss target (4 minutes apart).
1355-1410	4 MK 83 bombs dropped – 3 hit target, 1 misses target (5 minutes apart).
1500	Surface gunfire commences – 400 5-inch rounds fired (one every 6 seconds), 280 hit target, 120 miss target.
1700	MK 48 Torpedo fired, hits, and sinks target.

D.3 ENVIRONMENTAL PROVINCES

Propagation loss ultimately determines the extent of the Zone of Influence (ZOI) for a particular source activity. In turn, propagation loss as a function of range responds to a number of environmental parameters:

- Water depth
- Sound speed variability throughout the water column
- Bottom geo-acoustic properties, and
- Surface roughness, as determined by wind speed

Due to the importance that propagation loss plays in Anti-Submarine Warfare (ASW) exercises, the Navy has, over the last four to five decades, invested heavily in measuring and modeling these environmental parameters. The result of this effort is the following collection of global databases of these environmental parameters, which are accepted as standards for Navy modeling efforts.

- Water depth - Digital Bathymetry Data Base Variable Resolution (DBDBV)
- Sound speed - Generalized Digital Environmental Model (GDEM)
- Bottom loss - Low-Frequency Bottom Loss (LFBL), Sediment Thickness Database, and High-Frequency Bottom Loss (HFBL), and
- Wind speed - U.S. Navy Marine Climatic Atlas of the World

This section provides a discussion of the relative impact of these various environmental parameters. These examples then are used as guidance for determining environmental provinces (that is, regions in which the environmental parameters are relatively homogeneous and can be represented by a single set of environmental parameters) within the TMAA.

D.3.1 Impact of Environmental Parameters

Within a typical operating area, the environmental parameter that tends to vary the most is bathymetry. It is not unusual for water depths to vary by an order of magnitude or more, resulting in significant impacts upon the ZOI calculations. Bottom loss can also vary considerably over typical operating areas but its impact upon ZOI calculations tends to be limited to waters on the continental shelf and the upper portion of the slope. Generally, the primary propagation paths in deep water, from the source to most of the ZOI volume, do not involve any interaction with bottom. In shallow water, particularly if the sound velocity profile directs all propagation paths to interact with the bottom, bottom loss variability can play a larger role.

The spatial variability of the sound speed field is generally small over operating areas of typical size. The presence of a strong oceanographic front is a noteworthy exception to this rule. To a lesser extent, variability in the depth and strength of a surface duct can be of some importance. In the mid-latitudes, seasonal variation often provides the most significant variation in the sound speed field. For this reason, both summer and winter profiles are modeled for each selected environment.

D.3.2 Environmental Provincing Methodology

The underwater acoustic environment can be quite variable over ranges in excess of ten kilometers. For ASW applications, ranges of interest are often sufficiently large as to warrant the modeling of the spatial variability of the environment. In the propagation loss calculations, each of the environmental parameters is allowed to vary (either continuously or discretely) along the path from acoustic source to receiver. In such applications, each propagation loss calculation is conditioned upon the particular locations of the source and receiver.

On the other hand, the range of interest for marine animal harassment by most Naval activities is more limited. This reduces the importance of the exact location of source and marine animal and makes the modeling required more manageable in scope.

In lieu of trying to model every environmental profile that can be encountered in an operating area, this effort utilizes a limited set of representative environments. Each environment is characterized by a fixed water depth, sound velocity profile, and bottom loss type. The operating area is then partitioned into homogeneous regions (or provinces) and the most appropriately representative environment is assigned to each. This process is aided by some initial provincing of the individual environmental parameters. The Navy-standard high-frequency bottom loss database in its native form is globally partitioned into nine classes. Low-frequency bottom loss is likewise provinced in its native form, although it is not considered in the process of selecting environmental provinces. Only the broadband sources produce acoustic energy at the frequencies of interest for low-frequency bottom loss (typically less than 1 kHz); even for those sources the low-frequency acoustic energy is secondary to the energy above 1 kHz. The Navy-standard sound velocity profiles database is also available as a provinced subset. Only the Navy-standard bathymetry database varies continuously over the world’s oceans. However, even this environmental parameter is easily provinced by selecting a finite set of water depth intervals. For this analysis “octave-spaced” intervals (10, 20, 50, 100, 200, 500, 1000, 2000, and 5000 m) provide an adequate sampling of water depth dependence.

ZOI volumes are then computed using propagation loss estimates derived for the representative environments. Finally, a weighted average of the ZOI volumes is taken over all representative environments; the weighting factor is proportional to the geographic area spanned by the environmental province.

The selection of representative environments is subjective. However, the uncertainty introduced by this subjectivity can be mitigated by selecting more environments and by selecting the environments that occur most frequently over the operating area of interest.

As discussed in the previous subsection, ZOI estimates are most sensitive to water depth. Unless otherwise warranted, at least one representative environment is selected in each bathymetry province. Within a bathymetry province, additional representative environments are selected as needed to meet the following requirements.

- In shallow water (less than 1,000 meters), bottom interactions occur at shorter ranges and more frequently; thus significant variations in bottom loss need to be represented.
- Surface ducts provide an efficient propagation channel that can greatly influence ZOI estimates. Variations in the mixed layer depth need to be accounted for if the water is deep enough to support the full extent of the surface duct.

Depending upon the size and complexity of the operating area, the number of environmental provinces tends to range from 5 to 20.

D.3.3 Description of Environmental Provinces

The TMAA is approximately 92,246 square kilometers of ocean located south of Prince William Sound and east of Kodiak Island. The TMAA encompasses Warning Area W-612 and extends from the continental shelf to the deep waters of the Gulf of Alaska. The acoustic sources described in subsection D2 are deployed throughout the TMAA. This subsection describes the representative environmental provinces selected for the GOA. For all of these provinces, the average wind speed in the winter is 19 knots and in the summer 12 knots.

The GOA contains a total of 20 distinct environmental provinces. These represent various combinations of six bathymetry provinces, two Sound Velocity Profile (SVP) provinces, and four High-Frequency Bottom Loss (HFBL) classes.

The bathymetry provinces represent depths ranging from 100 meters to typical deep-water depths (slightly more than 5,000 meters). Nearly two-thirds of the Exercise Area is characterized as deep-water (depths of 2,000 meters or more). The second most prevalent water depth, covering nearly one-quarter of the Exercise Area, is representative of waters near the continental shelf break. The remaining water depths provide only small contributions (individually less than 5%) to the analysis. The distribution of the bathymetry provinces over the GOA is provided in D-7.

Table D-7 – Distribution of Bathymetry Provinces in GOA

Province Depth (m)	Frequency of Occurrence
100	4.85 %
200	22.29 %
500	4.22 %
1000	4.53 %
2000	12.67 %
5000	51.44 %

The distribution of the two sound speed provinces found in the TMAA is presented in Table D-8.

Table D-8 – Distribution of Sound Speed Provinces in GOA

SVP Province	Frequency of Occurrence
21	30.46 %
22	69.54 %

The variation in sound speed profiles associated with these two provinces is significant. This is illustrated in Figure D-1 and D-2 that display the upper 1,000 meters of the winter and summer profiles, respectively. In the winter, province 21 is a classic half-channel profile. The strong near-surface (within the upper 200 meters) gradient is the likely product of thorough mixing by strong winter winds and some fresh water sources. The winter profile for province 22 features a strong surface duct to a depth of 100 meters, also the result of thorough mixing by the winter winds. In contrast to province 21, however, the surface layer is modestly warmer. Nonetheless, both profiles are conducive to favorable sound propagation from a near-surface source.

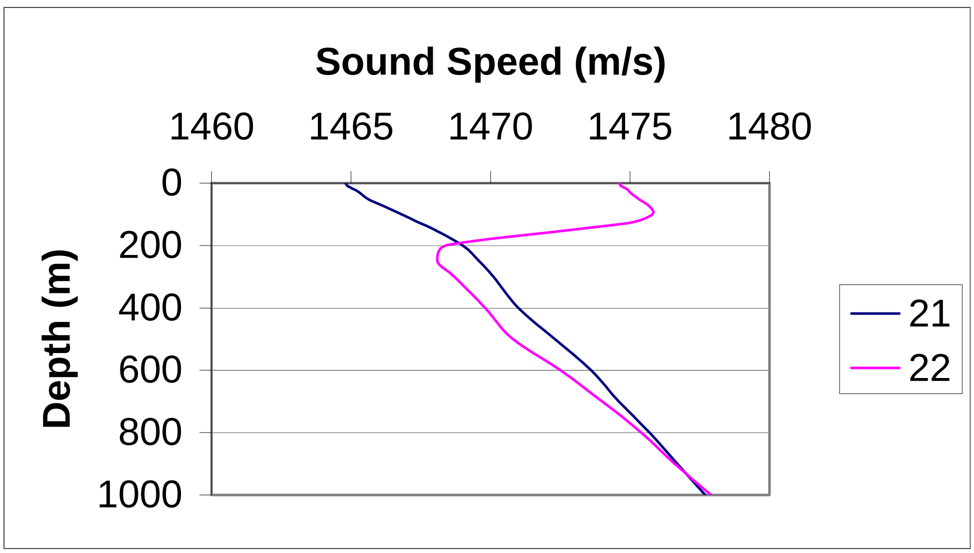

Figure D-1. – Winter SVPs in GOA

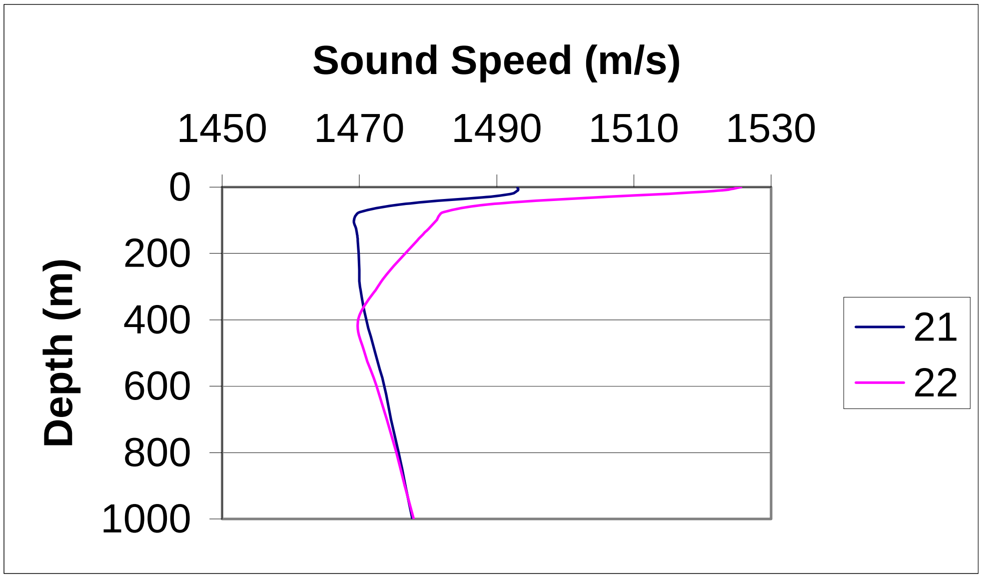

Figure D-2. – Summer SVPs in GOA

The summer profiles exhibit an even wider range of differences in the upper 200 meters (as much as 25 m/sec at the surface) with neither featuring a surface duct of significance. In the absence of surface loss considerations, both summer profiles would be less favorable than their winter counterparts for propagation from a near-surface source. However, the high wind speeds that are prevalent in the winter and the upward-refracting nature of the winter profiles appear to produce significantly higher surface scattering losses which can lead to summer being the season with the more favorable propagation.

The four HFBL classes represented in the GOA vary from low-loss bottoms (class 2, typically in shallow water) to high-loss bottoms (class 8). The four classes are fairly equally distributed as indicated in Table D-9 Distribution of High-Frequency Bottom Loss Classes in GOA. However, since two (classes 2 and 3) of the four classes are relatively low-loss, the bias in the environmental provinces will be towards low-loss bottoms.

Table D-9 – Distribution of High-Frequency Bottom Loss Classes in GOA

HFBL Class	Frequency of Occurrence
2	28.28 %
3	22.60 %
5	22.70 %
8	26.42 %

The logic for consolidating the environmental provinces focuses upon water depth, using the sound speed profile (in deep water) and the HFBL class (in shallow water) as secondary differentiating factors. The first consideration was to ensure that all six bathymetry provinces are represented. Then within each bathymetry province further partitioning of provinces proceeded as follows:

- The three shallowest bathymetry provinces are each represented by one environmental province. In each case, the bathymetry province is dominated (in some cases almost exclusively) by a single HFBL class, so that the secondary differentiating environmental parameter is of no consequence.
- The 1000-meter bathymetry province has two environmental provinces (differing in SVP province only) that occur in small, but relatively equal portions. Although they collectively

represent less than 5% of the TMAA, both are included in the analysis to ensure thoroughness. A third environmental province with a different HFBL class is not encountered enough to warrant consideration.

- The 2000-meter bathymetry province contains two environmental provinces that feature different SVP provinces. Both occur with sufficient frequency to warrant inclusion in the analysis.
- The 5000-meter bathymetry province consists of five environmental provinces. Four of these provinces are maintained for analysis; the fifth province is representative of less than one percent of the TMAA and for that reason, is excluded from consideration.

The distribution of the resulting eleven environmental provinces used in the acoustic modeling is summarized in Table D-10 and depicted in Figure D-3.

Table D-10 – Distribution of Environmental Provinces in TMAA

Environmental Province	Water Depth	SVP Province	Frequency of Occurrence
1	100 m	21	4.85 %
2	200 m	21	22.29 %
3	500 m	21	4.22 %
4	1000 m	21	2.32 %
5	1000 m	22	2.21 %
6	2000 m	21	10.61 %
7	2000 m	22	2.06 %
8	5000 m	21	22.60 %
9	5000 m	21	21.20 %
10	5000 m	22	1.51 %
11	5000 m	21	6.13 %

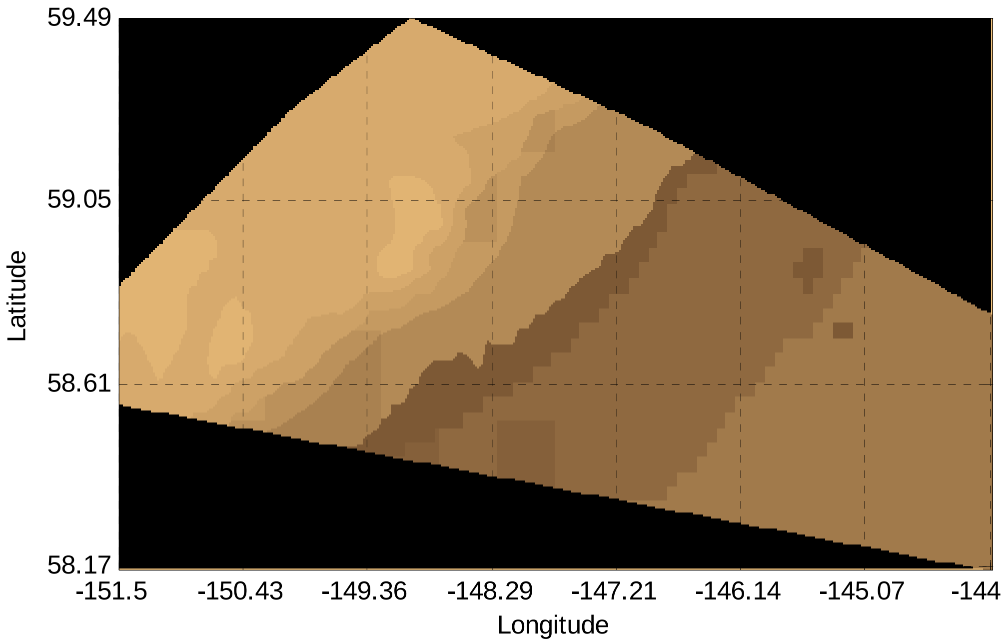

Figure D-3. – Distribution of Environmental Provinces in the TMAA

On this plot, darker-colored regions correspond to higher environmental province numbers, and hence depict deeper regions of the TMAA.

SINKEX operations are restricted to areas outside of 50 nautical miles (nm) from land and in waters deeper than 1,000 fathoms (or 1,852 meters). These limitations result not only in a smaller set of environments for analysis but also different frequencies of occurrence as indicated in Table D-11.

Table D-11 – Distribution of Environmental Provinces in the TMAA SINKEX Area

Environmental Province	Water Depth	SVP Province	Sediment Thickness	Frequency of Occurrence
1	2000 m	21	0.2 secs	7.15 %
2	5000 m	21	0.94 secs	35.55 %
3	5000 m	21	0.29 secs	9.04 %
4	5000 m	21	0.81 secs	45.93 %
5	5000 m	22	0.92 secs	1.75 %
6	5000 m	22	0.67 secs	0.58 %

D.4 IMPACT VOLUMES AND IMPACT RANGES

Many naval actions include the potential to injure or harass marine animals in the neighboring waters through noise emissions. The number of animals exposed to potential harassment in any such action is dictated by the propagation field and the characteristics of the noise source.

The impact volume associated with a particular activity is defined as the volume of water in which some acoustic metric exceeds a specified threshold. The product of this impact volume with a volumetric animal density yields the expected value of the number of animals exposed to that acoustic metric at a level that exceeds the threshold. The acoustic metric can either be an energy term (energy flux density, either in a limited frequency band or across the full band) or a pressure term (such as peak pressure or positive impulse). The thresholds associated with each of these metrics define the levels at which half of the animals exposed will experience some degree of harassment (ranging from behavioral change to mortality).

Impact volume is particularly relevant when trying to estimate the effect of repeated source emissions separated in either time or space. Impact range, which is defined as the maximum range at which a particular threshold is exceeded for a single source emission, defines the range to which marine mammal activity is monitored in order to meet mitigation requirements.

With the exception of explosive sources, the sole relevant measure of potential harm to the marine wildlife due to sonar operations is the accumulated (summed over all source emissions) energy flux density received by the animal over the duration of the activity. Harassment measures for explosive sources include energy flux density and pressure-related metrics (peak pressure and positive impulse).

Regardless of the type of source, estimating the number of animals that may be injured or otherwise harassed in a particular environment entails the following steps.

- Each source emission is modeled according to the particular operating mode of the sonar. The "effective" energy source level is computed by integrating over the bandwidth of the source, scaling by the pulse length, and adjusting for gains due to source directivity. The location of the source at the time of each emission must also be specified.

- For the relevant environmental acoustic parameters, transmission loss (TL) estimates are computed, sampling the water column over the appropriate depth and range intervals. TL data are sampled at the typical depth(s) of the source and at the nominal center frequency of the source. If the source is relatively broadband, an average over several frequency samples is required.
- The accumulated energy within the waters that the source is "operating" is sampled over a volumetric grid. At each grid point, the received energy from each source emission is modeled as the effective energy source level reduced by the appropriate propagation loss from the location of the source at the time of the emission to that grid point and summed. For the peak pressure or positive impulse, the appropriate metric is similarly modeled for each emission. The maximum value of that metric, over all emissions, is stored at each grid point.
- The impact volume for a given threshold is estimated by summing the incremental volumes represented by each grid point for which the appropriate metric exceeds that threshold.
- Finally, the number of harassments is estimated as the "product" (scalar or vector, depending upon whether an animal density depth profile is available) of the impact volume and the animal densities.

This section describes in detail the process of computing impact volumes (that is, the first four steps described above). This discussion is presented in two parts: active sonars and explosive sources. The relevant assumptions associated with this approach and the limitations that are implied are also presented. The final step, computing the number of harassments is discussed in subsection D.6.

D.4.1 Computing Impact Volumes for Active Sound Sources

This section provides a detailed description of the approach taken to compute impact volumes for active sonars. Included in this discussion are:

- Identification of the underwater propagation model used to compute transmission loss data, a listing of the source-related inputs to that model, and a description of the output parameters that are passed to the energy accumulation algorithm.
- Definitions of the parameters describing each sonar type.
- Description of the algorithms and sampling rates associated with the energy accumulation algorithm.

D.4.1.1 Transmission Loss Calculations

Transmission loss (TL) data are pre-computed for each of two seasons in each of the environmental provinces described in the previous subsection using the Gaussian Ray Bundle (GRAB) propagation loss model (Keenan, 2000). The TL output consists of a parametric description of each significant eigenray (or propagation path) from source to animal. The description of each eigenray includes the departure angle from the source (used to model the source vertical directivity later in this process), the propagation time from the source to the animal (used to make corrections to absorption loss for minor differences in frequency and to incorporate a surface-image interference correction at low frequencies), and the transmission loss suffered along the eigenray path.

The frequency and source depth TL inputs are specified in Table D-12.

Table D-12 – TL Frequency and Source Depth by Type

SONAR	FREQUENCY	SOURCE DEPTH
SQS-53	3.5 kHz	7 m
AQS-22	4.1 kHz	27 m
ASQ-62	8 kHz	27 m
SQS-56	7.5 kHz	7 m
MK-84 Range Pingers	12.9 kHz	7m, 100m
PUTR Transponders	8.8 kHz	1,800 m
MK-39 EMATT	900 Hz	100 m
BQQ-10	Classified	100 m
BQS-15	Classified	50 m
SUS, MK-84	3.4 kHz	50 m

The eigenray data for a single GRAB model run are sampled at uniform increments in range out to a maximum range for a specific "animal" (or "target" in GRAB terminology) depth. Multiple GRAB runs are made to sample the animal depth dependence. The depth and range sampling parameters are summarized in Table D-13. Note that some of the low-power sources do not require TL data to large maximum ranges.

Table D-13 – TL Depth and Range Sampling Parameters by Sonar Type

SONAR	RANGE STEP	MAXIMUM RANGE	DEPTH SAMPLING
SQS-53	10 m	200 km	0 – 1 km in 5 m steps 1 km – Bottom in 10 m steps
AQS-22	10 m	10 km	0 – 1 km in 5 m steps 1 km – Bottom in 10 m steps
ASQ-62	5 m	5 km	0 – 1 km in 5 m steps 1 km – Bottom in 10 m steps
SQS-56	10 m	50 km	0 – 1 km in 5 m steps 1 km – Bottom in 10 m steps
MK-84 Range Pingers	5 m	15 km	0 – 1 km in 5 m steps 1 km – Bottom in 10 m steps
PUTR Transponders	5 m	15 km	0 – 1 km in 5 m steps 1 km – Bottom in 10 m steps
MK-39 EMATT	5 m	1 km	1 m steps
BQQ-10	Classified	Classified	0 – 1 km in 5 m steps 1 km – Bottom in 10 m steps
BQS-15	Classified	Classified	0 – 1 km in 5 m steps 1 km – Bottom in 10 m steps
SUS, MK-84	5 m	1 km	1 m steps

In a few cases, most notably the SQS-53 for levels below approximately 180 dB, TL data may be required by the energy summation algorithm at ranges greater than covered by the pre-computed GRAB data. In these cases, TL is extrapolated to the required range using a simple cylindrical spreading loss law in addition to the appropriate absorption loss. This extrapolation leads to a conservative (or under) estimate of transmission loss at the greater ranges.

Although GRAB provides the option of including the effect of source directivity in its eigenray output, this capability is not exercised. By preserving data at the eigenray level, this allows source directivity to be applied later in the process and results in fewer TL calculations.

The other important feature that storing eigenray data supports is the ability to model the effects of surface-image interference that persist over range. However, this is primarily important at frequencies lower than those associated with the sonars considered in this subsection. A detailed description of the modeling of surface-image interference is presented in the subsection on explosive sources.

D.4.1.2 Energy Summation

The summation of energy flux density over multiple pings in a range-independent environment is a trivial exercise for the most part. A volumetric grid that covers the waters in and around the area of sonar operation is initialized. The source then begins its set of pings. For the first ping, the TL from the source to each grid point is determined (summing the appropriate eigenrays after they have been modified by the vertical beam pattern), the "effective" energy source level is reduced by that TL, and the result is added to the accumulated energy flux density at that grid point. After each grid point has been updated, the accumulated energy at grid points in each depth layer is compared to the specified threshold. If the accumulated energy exceeds that threshold, then the incremental volume represented by that grid point is added to the impact volume for that depth layer. Once all grid points have been processed, the resulting sum of the incremental volumes represents the impact volume for one ping.

The source is then moved along one of the axes in the horizontal plane by the specified ping separation range and the second ping is processed in a similar fashion. Again, once all grid points have been processed, the resulting sum of the incremental volumes represents the impact volume for two pings. This procedure continues until the maximum number of pings specified has been reached.

Defining the volumetric grid over which energy is accumulated is the trickiest aspect of this procedure. The volume must be large enough to contain all volumetric cells for which the accumulated energy is likely to exceed the threshold but not so large as to make the energy accumulation computationally unmanageable.

Determining the size of the volumetric grid begins with an iterative process to determine the lateral extent to be considered. Unless otherwise noted, throughout this process the source is treated as omni-directional and the only animal depth that is considered is the TL target depth that is closest to the source depth (placing source and receiver at the same depth is generally an optimal TL geometry).

The first step is to determine the impact range (R_{max}) for a single ping. The impact range in this case is the maximum range at which the effective energy source level reduced by the transmission loss is greater than the threshold. Next, the source is moved along a straight-line track and energy flux density is accumulated at a point that has a CPA range of R_{max} at the mid-point of the source track. That total energy flux density summed over all pings is then compared to the prescribed threshold. If it is greater than the threshold (which, for the first R_{max}, it must be) then R_{max} is increased by ten percent, the accumulation process is repeated, and the total energy is again compared to the threshold. This continues until R_{max} grows large enough to ensure that the accumulated energy flux density at that lateral range is less than the threshold. The lateral range dimension of the volumetric grid is then set at twice R_{max}, with the grid centered along the source track. In the direction of advance for the source, the volumetric grid extends on the interval from [$-R_{max}$, 3 R_{max}] with the first source position located at zero in this dimension. Note that the source motion in this direction is limited to the interval [0, 2 R_{max}]. Once the source reaches 2 R_{max} in this direction, the incremental volume contributions have approximately reached their asymptotic limit and further pings add essentially the same amount. This geometry is demonstrated in Figure D-4 below.

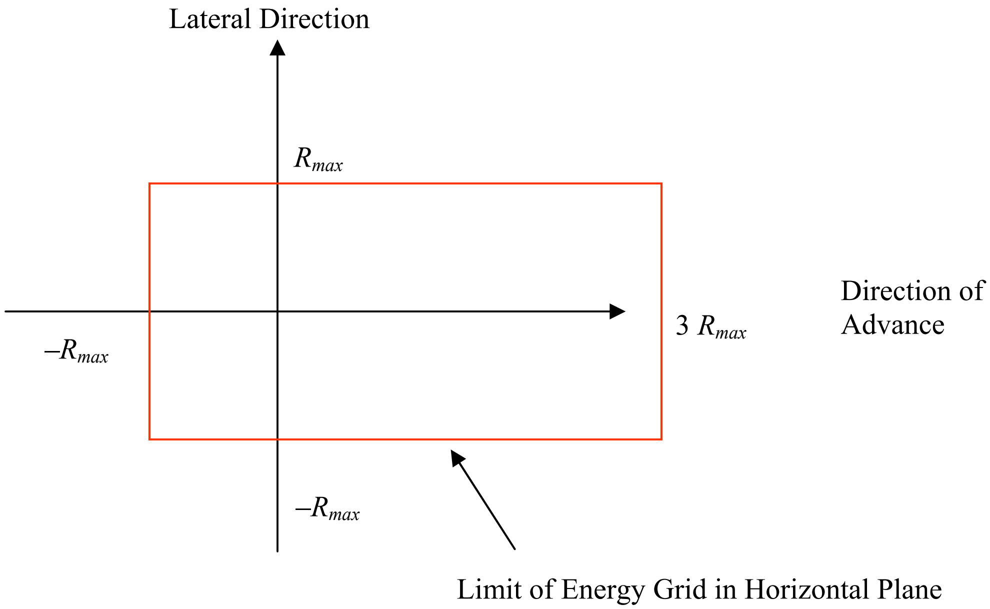

Figure D-4. Horizontal Plane of Volumetric Grid for Omni Directional Source

If the source is directive in the horizontal plane, then the lateral dimension of the grid may be reduced and the position of the source track adjusted accordingly. For example, if the main lobe of the horizontal source beam is limited to the starboard side of the source platform, then the port side of the track is reduced substantially as demonstrated in Figure D-5.

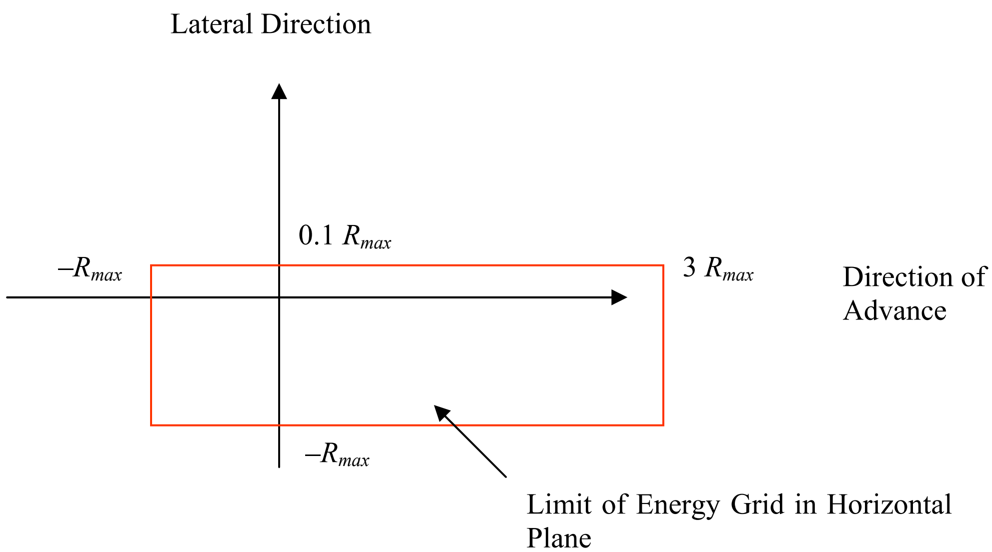

Figure D-5. Horizontal Plane of Volumetric Grid for Starboard Beam Source

Once the extent of the grid is established, the grid sampling can be defined. In both dimensions of the horizontal plane the sampling rate is approximately $R_{max}/100$. The round-off error associated with this sampling rate is roughly equivalent to the error in a numerical integration to determine the area of a circle with a radius of R_{max} with a partitioning rate of $R_{max}/100$ (approximately one percent). The depth-sampling rate of the grid is comparable to the sampling rates in the horizontal plane but discretized to match an actual TL sampling depth. The depth-sampling rate is also limited to no more than ten meters to ensure that significant TL variability over depth is captured.

D.4.1.3 Impact Volume per Hour of Source Operation

The impact volume for a source moving relative to the animal population increases with each additional ping. The rate at which the impact volume increases varies with a number of parameters but eventually approaches some asymptotic limit. Beyond that point the increase in impact volume becomes essentially linear as depicted in Figure D-6 using the SQS-53 as an example.

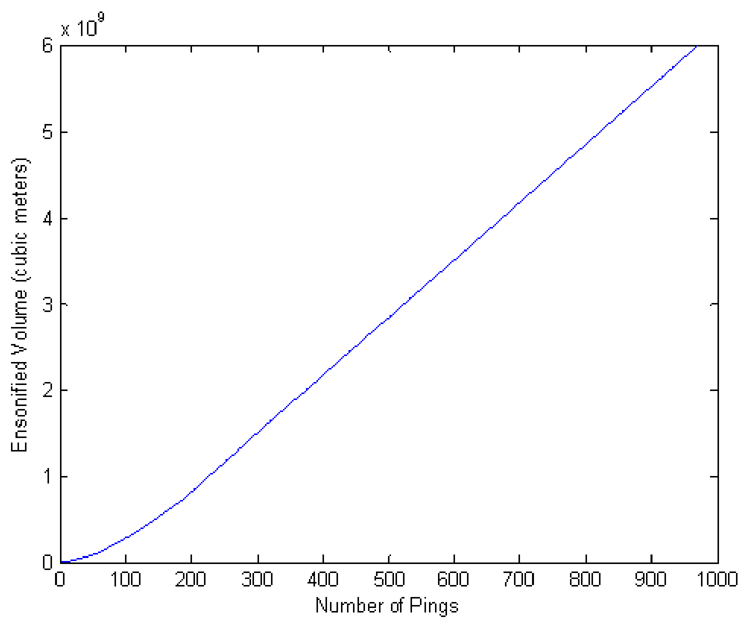

Figure D-6. SQS-53 Impact Volume by Ping

The slope of the asymptotic limit of the impact volume at a given depth is the impact volume added per ping. This number multiplied by the number of pings in an hour gives the hourly impact volume for the given depth increment. Completing this calculation for all depths in a province, for a given source, gives the hourly impact volume vector, v_n, which contains the hourly impact volumes by depth for province *n*. Figure D-7 provides an example of an hourly impact volume vector for a particular environment.

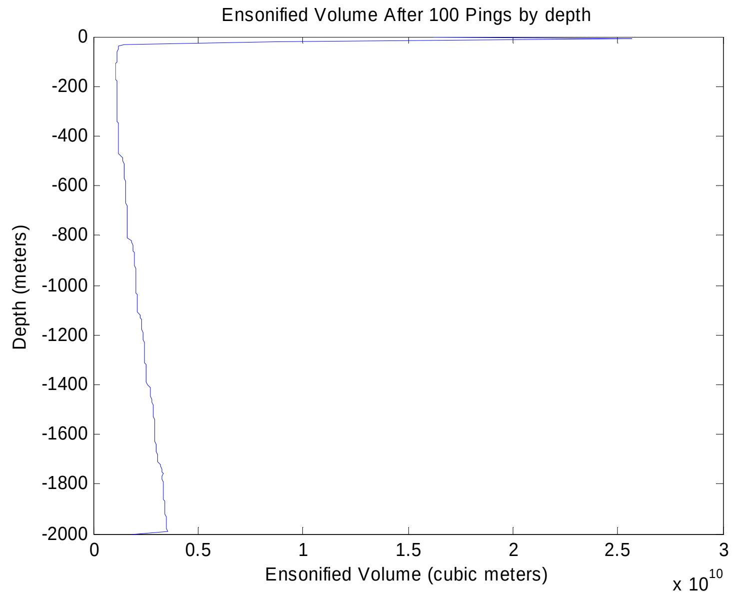

Figure D-7. Example of an Impact Volume Vector

D.4.2 Computing Impact Volumes for Explosive Sources

This section provides the details of the modeling of the explosive sources. This energy summation algorithm is similar to that used for sonars, only differing in details such as the sampling rates and source parameters. These differences are summarized in the following subsections. A more significant difference is that the explosive sources require the modeling of additional pressure metrics: (1) peak pressure, and (2) "modified" positive impulse. The modeling of each of these metrics is described in detail in the subsections of D.4.2.3.

D.4.2.1 Transmission Loss Calculations

Modeling impact volumes for explosive sources span requires the same type of TL data as needed for active sonars. However unlike active sonars, explosive ordnances and the EER source are broadband, contributing significant energy from tens of Hertz to tens of kilohertz. To accommodate the broadband nature of these sources, TL data are sampled at seven frequencies from 10 Hz to 40 kHz, spaced every two octaves.

An important propagation consideration at low frequencies is the effect of surface-image interference. As either source or target approach the surface, pairs of paths that differ by a single surface reflection set up an interference pattern that ultimately causes the two paths to cancel each other when the source or target is at the surface. A fully coherent summation of the eigenrays produces such a result but also introduces extreme fluctuations that would have to be highly sampled in range and depth, and then smoothed to give meaningful results. An alternative approach is to implement what is sometimes called a semi-coherent summation. A semi-coherent sum attempts to capture significant effects of surface-image interference (namely the reduction of the field due to destructive interference of reflected paths as the source or target approach the surface) without having to deal with the more rapid fluctuations associated with a fully coherent sum. The semi-coherent sum is formed by a random phase addition of paths that have already been multiplied by the expression:

$$\sin^2\left(\frac{4\pi f z_s z_a}{c^2 t}\right)$$

where f is the frequency, z_s is the source depth, z_a is the animal depth, c is the sound speed and t is the travel time from source to animal along the propagation path. For small arguments of the sine function this expression varies directly as the frequency and the two depths. It is this relationship that causes the propagation field to go to zero as the depths approach the surface or the frequency approaches zero.

This surface-image interference must be applied across the entire bandwidth of the explosive source. The TL field is sampled at several representative frequencies. However, the image-interference correction given above varies substantially over that frequency spacing. To avoid possible under sampling, the image-interference correction is averaged over each frequency interval.

D.4.2.2 Source Parameters

Unlike active sonars, explosive sources are defined by only two parameters: (1) net explosive weight, and (2) source detonation depth. Values for these source parameters are defined earlier in subsection D.2.2.

The effective energy source level, which is treated as a de facto input for the other sources, is instead modeled directly for SSQ-110 explosive sonobuoys and munitions. For both, the energy source level is comparable to the model used for other explosives (Arons (1954), Weston (1960), McGrath (1971), Urick (1983), Christian and Gaspin (1974)). The energy source level over a one-third octave band with a center frequency of f for a source with a net explosive weight of w pounds is given by:

$$\text{ESL} = 10 \log_{10} (0.26 f) + 10 \log_{10} (2 p_{max}^2 / [1/\theta^2 + 4 \pi f^2]) + 197 \text{ dB}$$

where the peak pressure for the shock wave at 1 meter is defined as

$$p_{max} = 21600 (w^{1/3} / 3.28)^{1.13} \text{ psi} \qquad \text{(A-1)}$$

and the time constant is defined as:

$$\theta = [(0.058) (w^{1/3}) (3.28 / w^{1/3})^{0.22}] / 1000 \text{ msec} \qquad \text{(A-2)}$$

In contrast to munitions that are modeled as omni-directional sources, the SSQ-110 is a directed source consisting of two explosive strips that are fired simultaneously from the center of the array. Each strip generates a beam pattern with the steer direction of the main lobe determined by the burn rate. The resulting response of the entire array is a bifurcated beam for frequencies above 200 Hz, while at lower frequencies the two beams tend to merge into one.

Since very short ranges are under consideration, the loss of directivity of the array needs to be accounted for in the near field of the array. This is accomplished by modeling the sound pressure level across the field as the coherent sum of contributions of infinitesimal sources along the array that are delayed according to the burn rate. For example, for frequency f the complex pressure contribution at a depth z and horizontal range r from an infinitesimal source located at a distance z' above the center of the array is

$$p(r,z) = e^{i\phi}$$

where

$\phi = kr' + \alpha z'$, and

$\alpha = 2\,\pi f\,/\,c_b$

with k the acoustic wave number, c_b the burn rate of the explosive ribbon, and r' the slant range from the infinitesimal source to the field point (x,z).

Beam patterns as function of vertical angle are then sampled at various ranges out to a maximum range that is approximately L^2 / λ where L is the array length and λ is the wavelength. This maximum range is a rule-of-thumb estimate for the end of the near field (Bartberger, 1965). Finally, commensurate with the resolution of the TL samples, these beam patterns are averaged over octave bands.

A couple of sample beam patterns are provided in Figure D-8 and Figure D-9. In both cases, the beam response is sampled at various ranges from the source array to demonstrate the variability across the near field. The 80-Hz family of beam patterns presented in Figure D-8 shows the rise of a single main lobe as range increases.

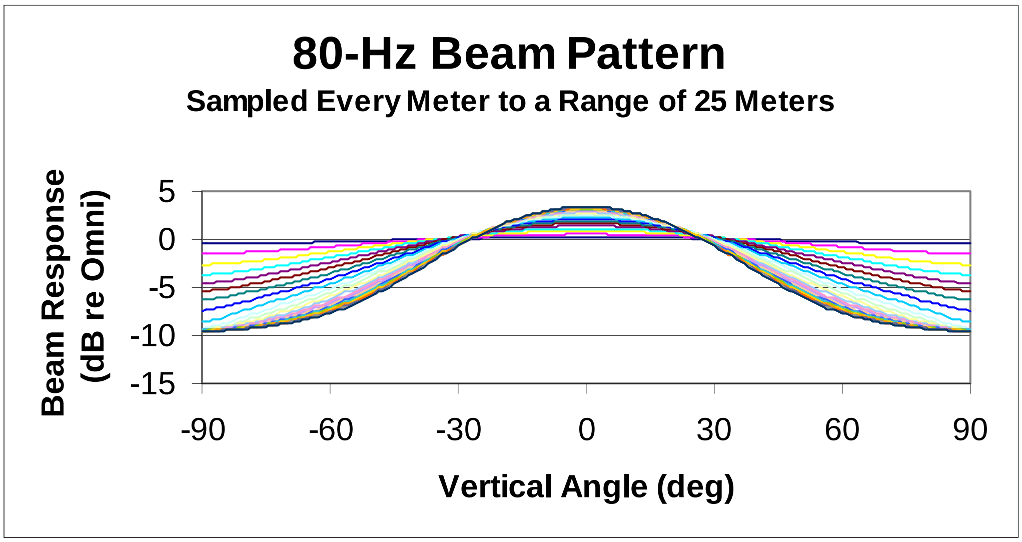

Figure D-8. 80-Hz Beam Patterns across Near Field of EER Source

On the other hand, the 1,250-Hz family of beam patterns depicted in Figure D-9 demonstrates the typical high-frequency bifurcated beam.

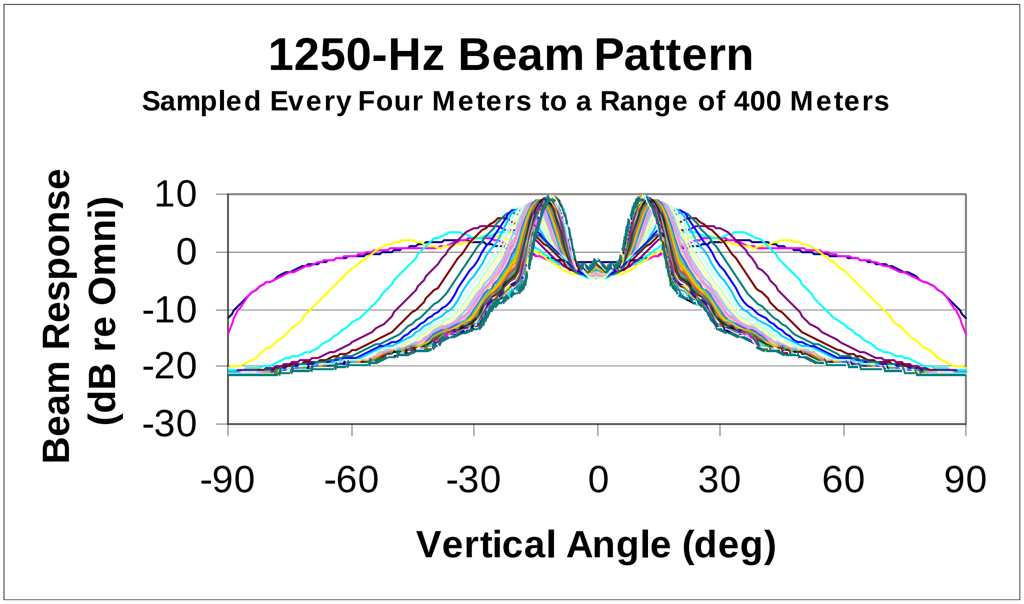

Figure D-9. 1250-Hz Beam Patterns across Near Field of SSQ-110 Source

D.4.2.3 Impact Volumes for Various Metrics

The impact of explosive sources on marine wildlife is measured by three different metrics, each with its own thresholds. The energy metric, peak one-third octave, is treated in similar fashion as the energy metric used for the active sonars, including the summation of energy if there are multiple source emissions. The other two, peak pressure and positive impulse, are not accumulated but rather the maximum levels are taken.

Peak One-Third Octave Energy Metric

The computation of impact volumes for the energy metric closely follows the approach taken to model the energy metric for the active sonars. The only significant difference is that energy flux density is sampled at several frequencies in one-third-octave bands and only the peak one-third-octave level is accumulated over time.

Peak Pressure Metric

The peak pressure metric is a simple, straightforward calculation at each range/animal depth combination. First, the transmission ratio, modified by the source level in a one-octave band and the vertical beam pattern, is averaged across frequency on an eigenray-by-eigenray basis. This averaged transmission ratio (normalized by the total broadband source level) is then compared across all eigenrays with the maximum designated as the peak arrival. Peak pressure at that range/animal depth combination is then simply the product of:

- The square root of the averaged transmission ratio of the peak arrival,
- The peak pressure at a range of 1 meter (given by equation A-1), and
- The similitude correction (given by $r^{-0.13}$, where r is the slant range along the eigenray estimated as *tc* with *t* the travel time along the dominant eigenray and *c* the nominal speed of sound).

If the peak pressure for a given grid point is greater than the specified threshold, then the incremental volume for the grid point is added to the impact volume for that depth layer.

“Modified” Positive Impulse Metric

The modeling of positive impulse follows the work of Goertner (Goertner, 1982). The Goertner model defines a “partial” impulse as

$$\int_0^{T_{min}} p(t)\,\mathrm{d}t$$

where $p(t)$ is the pressure wave from the explosive as a function of time t, defined so that $p(t) = 0$ for $t < 0$. This pressure wave is modeled as

$$p(t) = p_{max}\, e^{-t/\theta}$$

where p_{max} is the peak pressure at 1 meter (see, equation B-1), and θ is the time constant defined as

$$\theta = 0.058\, w^{1/3}\, (r/w^{1/3})^{0.22} \text{ seconds}$$

with w the net explosive weight (pounds), and r the slant range between source and animal.

The upper limit of the “partial” impulse integral is

$$T_{min} = \min\,\{T_{cut}, T_{osc}\}$$

where T_{cut} is the time to cutoff and T_{osc} is a function of the animal lung oscillation period. When the upper limit is T_{cut}, the integral is the definition of positive impulse. When the upper limit is defined by T_{osc}, the integral is smaller than the positive impulse and thus is just a “partial” impulse. Switching the integral limit from T_{cut} to T_{osc} accounts for the diminished impact of the positive impulse upon the animals lungs that compress with increasing depth and leads to what is sometimes call a “modified” positive impulse metric.

The time to cutoff is modeled as the difference in travel time between the direct path and the surface-*reflected* path in an isospeed environment. At a range of r, the time to cutoff for a source depth z_s and an animal depth z_a is

$$T_{cut} = 1/c\ \{\ [r^2 + (z_a + z_s)^2]^{1/2} - [r^2 + (z_a - z_s)^2]^{1/2}\ \}$$

where c is the speed of sound.

The *animal* lung oscillation period is a function of animal mass M and depth z_a and is modeled as

$$T_{osc} = 1.17\, M^{1/3}\, (1 + z_a/33)^{-5/6}$$

where M is the animal mass (in kg) and z_a is the animal depth (in feet).

The modified positive impulse threshold is unique among the various injury and harassment metrics in that it is a function of depth and the animal weight. So instead of the user specifying the threshold, it is computed as $K\ (M/42)^{1/3}\ (1 + z_a/33)^{1/2}$. The coefficient K depends upon the level of exposure. For the onset of slight lung injury, K is 19.7; for the onset of extensive lung hemorrhaging (1% mortality), K is 47.

Although the thresholds are a function of depth and animal weight, sometimes they are summarized as their value at the sea surface for a typical dolphin calf (with an average mass of 12.2 kg). For the onset of slight lung injury, the threshold at the surface is approximately 13 psi-msec; for the onset of extensive lung hemorrhaging (1% mortality), the threshold at the surface is approximately 31 psi-msec.

As with peak pressure, the "modified" positive impulse at each grid point is compared to the derived threshold. If the impulse is greater than that threshold, then the incremental volume for the grid point is added to the impact volume for that depth layer.

D.4.2.4 Impact Volume per Explosive Detonation

The detonations of explosive sources are generally widely spaced in time and/or space. This implies that the impact volume for multiple firings can be easily derived by scaling the impact volume for a single detonation. Thus the typical impact volume vector for an explosive source is presented on a per-detonation basis.

D.4.3 Impact Volume by Region

The TMAA is described by eleven (11) environmental provinces. The hourly impact volume vector for operations involving any particular source is a linear combination of the eleven impact volume vectors with the weighting determined by the distribution of those eleven environmental provinces within the range. Unique hourly impact volume vectors for winter and summer are calculated for each type of source and each metric/threshold combination.

D.5 Risk Function: Theoretical and Practical Implementation

This section discusses the recent addition of a risk function response "threshold" to acoustic effects analysis procedure. This approach includes two parts, a metric, and a function to map exposure level under the metric to probability of harassment for acoustic sources. What these two parts mean, how they affect exposure calculations, and how they are implemented are the objects of discussion.

D.5.1 Thresholds and Metrics

The term "thresholds" is broadly used to refer to both thresholds and metrics. The difference, and the distinct roles of each in effects analyses, will be the foundation for understanding the dose-response approach, putting it in perspective, and showing that, conceptually, it is similar to past approaches.

Sound is a pressure wave, so at a certain point in space, sound is simply rapidly changing pressure. Pressure at a point is a function of time. Define $p(t)$ as pressure (in micropascals) at a given point at time t (in seconds); this function is called a "time series." Figure D-10 gives the time series of the first "hallelujah" in Handel's Hallelujah Chorus.

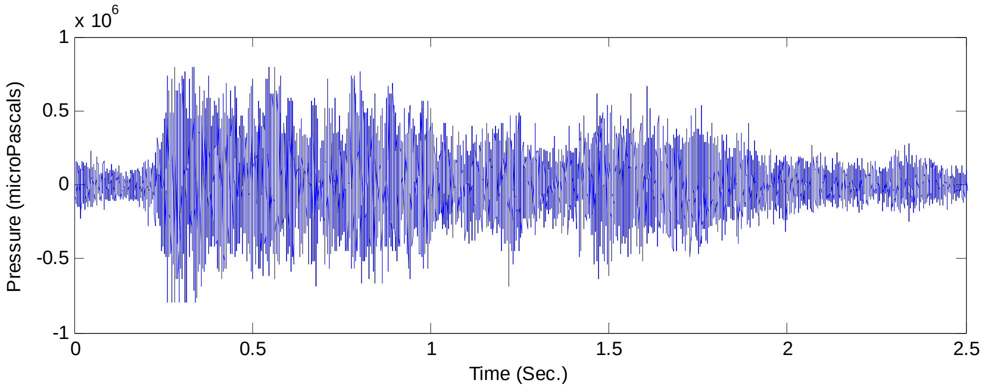

Figure D-10. Time Series

The time-series of a source can be different at different places. Therefore, sound, or pressure, is not only a function of time, but also of location. Let the function $p(t)$, then be expanded to p($t;x,y,z$) and denote the time series at point (x,y,z) in space. Thus, the series in Figure D-10 $p(t)$ is for a given point (x,y,z). At a different point in space, it would be different.

Assume that the location of the source is (0,0,0) and this series is recorded at (0,10,-4). The time series above would be p(t;0,10,-4) for 0<t<2.5.

As in Figure D-10, pressure can be positive or negative, but acoustic power, which is proportional to the square of the pressure, is always positive, this makes integration meaningful. Figure D-11 is $p^2(t;0,10,-4)$.

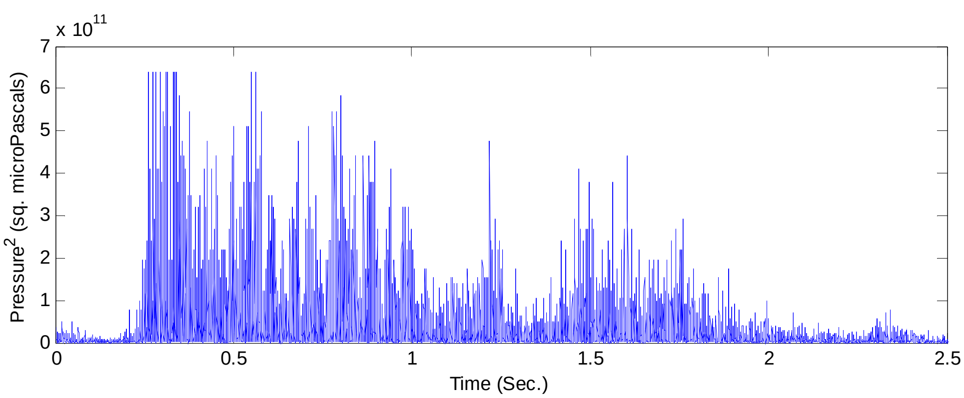

Figure D-11. Time Series Squared

The metric chosen to evaluate the sound field at the end of this first "hallelujah" determines how the time series is summarized from thousands of points, as in Figure D-10, to a single value for each point (x,y,z) in the space. The metric essentially "boils down" the four dimensional $p(t,x,y,z)$ into a three dimensional function $m(x,y,z)$ by dealing with time. There is more than one way to summarize the time component, so there is more than one metric.

D.5.2 Maximum Sound Pressure Level

Because of the large dynamic range of the acoustic power, it is generally represented on a logarithmic scale using sound pressure levels (SPLs). SPL is actually the ratio of acoustic power and density (power/unit area = $\frac{p^2}{Z}$ where Z = ρc is the acoustic impedance). This ratio is presented on a logarithmic scale relative to a reference pressure level, and is defined as:

$$SPL = 10\log_{10}\left(\frac{p^2}{p_{ref}^2}\right) = 20\log_{10}\left(abs\left(\frac{p}{p_{ref}}\right)\right)$$

(Note that SPL is defined in dB re a reference pressure, even though it comes from a ratio of powers.)

One way to characterize the power of the time series $p(t;x,y,z)$ with a single number over the 2.5 seconds is to only report the maximum SPL value of the function over time or,

$SPL_{\max} = \max\{10\log_{10}(p^2(t,x,y,z))\}$ (relative to a reference pressure of 1 µPa^2-s) for 0<t<2.5

The $SPL_{\max}$ for this snippet of the Hallelujah Chorus is $10\log_{10}(6.4\times10^{11}\,\mu Pa^2/1\mu Pa^2) = 118\,dB$ re 1µPa^2-s and occurs at 0.2606 seconds, as shown in Figure D-12.

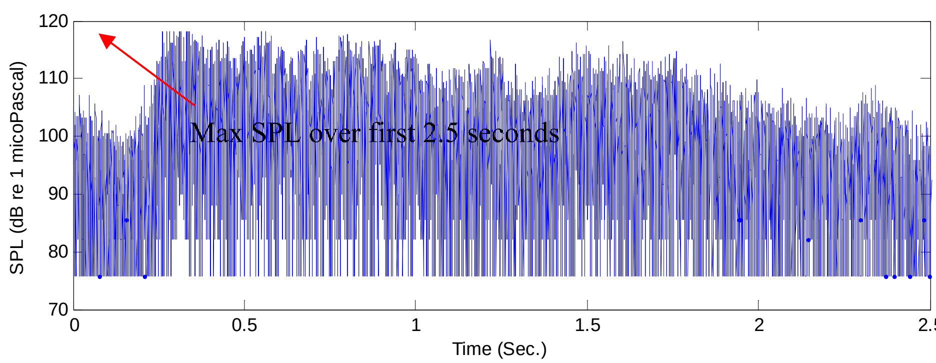

Figure D-12. Max SPL of Time Series Squared

D.5.3 Integration

$SPL_{\max}$ is not necessarily influenced by the duration of the sound (2.5 seconds in this case). Integrating the function over time gives the EFD, which accounts for this duration. A simple integration of $p^2(t;x,y,z)$ over t is common and is proportional to the EFD at (*x,y,z*). Because we will again be dealing in levels (logarithms of ratios), we neglect the impedance and simply measure the square of the pressure:

$$Energy = \int_0^T p^2(t,x,y,z)dt$$, where T is the maximum time of interest in this case 2.5.

The energy for this snippet of the Hallelujah Chorus is $8.47 \times 10^{10}\ \mu Pa^2 \cdot s$. This would more commonly be reported as an energy level (EL):

$$EL = 10\log_{10}\left(\frac{\int_0^T p^2(t,x,y,z)dt}{1.0\mu Pa^2 s}\right) = \text{ 109.3 dB re 1}\mu\text{Pa}^2\text{-s}$$

Energy is sometimes called "equal energy" because if *p*(*t*) is a constant function and the duration is doubled, the effect is the same as doubling the signal amplitude (*y* value). Thus, the duration and the signal have an "equal" influence on the energy metric.

Mathematically we have

$$\int_0^{2T} p(t)^2\,dt = 2\int_0^T p(t)^2\,dt = \int_0^T 2p(t)^2\,dt$$

or a doubling in duration equals a doubling in energy equals a doubling in signal.

Sometimes, the integration metrics are referred to as having a "3 dB exchange rate" because if the duration is doubled, this integral increases by a factor of two, or 10log10(2)=3.01 dB. Thus, equal energy has "a 3 dB exchange rate."

After *p(t)* is determined (i.e., when the stimulus is over), propagation models can be used to determine *p(t;x,y,z)* for every point in the vicinity and for a given metric. Define

$$m_a(x,y,z,T) = \text{value of metric "}a\text{" at point }(x,y,z)\text{ after time }T$$

So,

$$m_{energy}(x,y,z;T) = \int_0^T p(t)^2\,dt$$

$$m_{\max SPL}(x,y,z;T) = \max\ 10\log_{10}\left(p^2(t)\right)\ over\ \left[0,T\right]$$

Since modeling is concerned with the effects of an entire event, *T* is usually implicitly defined: a number that captures the duration of the event. This means that $m_a(x,y,z)$ is assumed to be measured over the duration of the received signal.

D.5.3.1 Three Dimensions versus Two Dimensions

To further reduce the calculation burden, it is possible to reduce the domain of $m_a(x,y,z)$ to two dimensions by defining $m_a(x,y) = \max\{m_a(x,y,z)\}$ over all *z*. This reduction is not used for this analysis, which is exclusively three-dimensional.

D.5.4 Threshold

For a given metric, a threshold is a function that gives the probability of exposure at every value of m_a. This threshold function will be defined as

$$D(m_a(x,y,z)) = P(\mathit{effect\ at}\ m_a(x,y,z))$$

The domain of *D* is the range of $m_a(x,y,z)$, and the range of *D* is [0,1].

An example of threshold functions is the heavyside (or unit step) function, currently used to determine permanent and temporary threshold shift (PTS and TTS) in cetaceans. For PTS, the metric is $m_{energy}(x,y,z)$, defined above, and the threshold function is a heavyside function with a discontinuity at 215 dB, shown in Figure D-13.

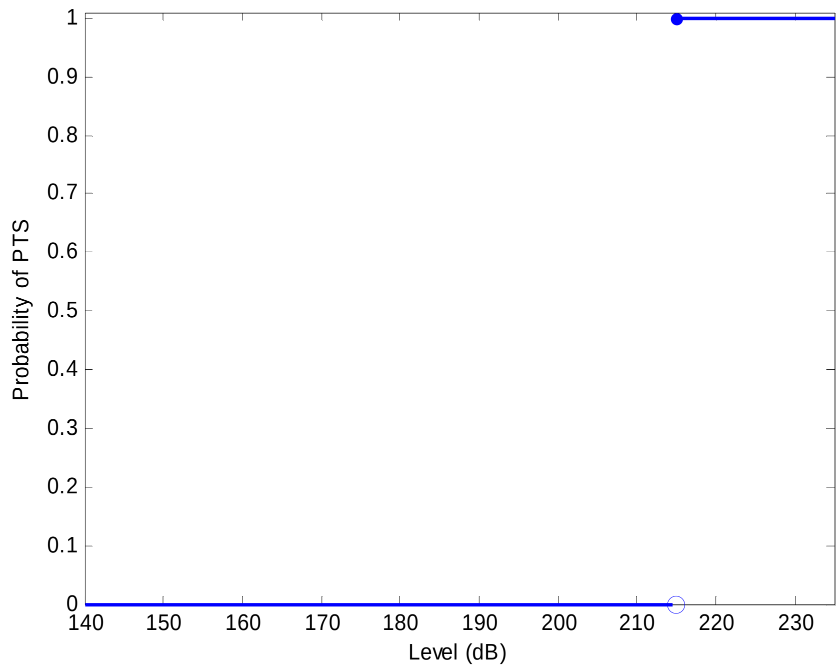

Figure D-13. PTS Heavyside Threshold Function

Symbolically, this *D* is defined as:

$$D(m_{energy}) = \begin{cases} 0 \ \mathit{for}\ m_{energy} < 215 \\ 1 \ \mathit{for}\ m_{energy} \geq 215 \end{cases}$$

Any function can be used for D, as long as its range is in [0,1]. The risk function uses normal Feller risk functions (defined below) instead of heavyside functions, and use the max SPL metric instead of the energy metric. While a heavyside function is specified by a single parameter, the discontinuity, a Feller function requires three parameters: the basement cutoff value, the level above the basement for 50% effect, and a steepness parameter. Mathematically, these Feller, "risk" functions, *D*, are defined as

$$D(m_{\max SPL}) = \begin{cases} \dfrac{1}{1+\left(\dfrac{K}{m_{\max SPL}-B}\right)^{A}} & for\ m_{\max SPL} \geq B \\ 0 & for\ m_{\max SPL} < B \end{cases}$$ [1]

where B = cutoff (or basement), K = the difference in level (dB) between the basement and the median (50% effect) harassment level, and A = the steepness factor. The dose function for odontocetes and pinnipeds uses the parameters:

B = 120 dB,

K = 45 dB, and

A = 10.

The dose function for mysticetes uses:

B = 120 dB,

K = 45 dB, and

A = 8.

Harbor porpoises are a special case. Though the metric for their behavioral harassment is also SPL, their risk function is a heavyside step function with a harassment threshold discontinuity (0 % to 100 %) at 120 dB. All other species use the continuous Feller risk-function for evaluating expected harassment.

D.5.5 Calculation of Expected Exposures

Determining the number of expected exposures for disturbance is the object of this analysis.

$$\text{Expected exposures in volume V} = \int_V \rho(V) D(m_a(V)) dV$$

For this analysis, $m_a = m_{\max SPL}$, so

$$\int_V \rho(V) D\big(m_a(V)\big) dV = \int_{-\infty}^{\infty}\int_{-\infty}^{\infty}\int_{-\infty}^{\infty} \rho(x,y,z) D(m_{\max SPL}(x,y,z))\, dx\, dy\, dz$$

In this analysis, the densities are constant over the *xy*-plane, and the *z* dimension is always negative, so this reduces to

$$\int_{-\infty}^{0} \rho(z) \int_{-\infty}^{\infty}\int_{-\infty}^{\infty} D(m_{\max SPL}(x,y,z))\, dx\, dy\, dz$$

1 The equation can also be represented as shown in Section 3.8.6.3 of this EIS/OEIS

D.5.6 Numeric Implementation

Numeric integration of $\int_{-\infty}^{0} \rho(z) \int_{-\infty}^{\infty}\int_{-\infty}^{\infty} D(m_{\max SPL}(x,y,z))\, dx\, dy\, dz$ can be involved because, although the bounds are infinite, *D* is non-negative out to 120 dB, which, depending on the environmental specifics, can drive propagation loss calculations and their numerical integration out to more than 100 km.

The first step in the solution is to separate out the *xy*-plane portion of the integral:

$$\text{Define } f(z) = \int_{-\infty}^{\infty}\int_{-\infty}^{\infty} D(m_{\max SPL}(x,y,z))\, dx\, dy .$$

Calculation of this integral is the most involved and time consuming part of the calculation. Once it is complete,

$$\int_{-\infty}^{0} \rho(z) \int_{-\infty}^{\infty}\int_{-\infty}^{\infty} D(m_{\max SPL}(x,y,z))\, dx\, dy\, dz = \int_{-\infty}^{0} \rho(z) f(z) dz ,$$

which, when numerically integrated, is a simple dot product of two vectors.

Thus, the calculation of *f(z)* requires the majority of the computation resources for the numerical integration. The rest of this section presents a brief outline of the steps to calculate *f(z)* and preserve the results efficiently.

The concept of numerical integration is, instead of integrating over continuous functions, to sample the functions at small intervals and sum the samples to approximate the integral. Smaller sized intervals yield closer approximations with longer calculation time, so a balance between accuracy and time is determined in the decision of step size. For this analysis, *z* is sampled in 5 meter steps to 1000 meters in depth and 10 meter steps to 2000 meters, which is the limit of animal depth in this analysis. The step size for *x* is 5 meters, and *y* is sampled with an interval that increases as the distance from the source increases. Mathematically,

$$z \in Z = \{0,5,...1000,1010,...,2000\}$$
$$x \in X = \{0,\pm5,...,\pm5k\}$$
$$y \in Y = \left\{0,\pm5*(1.005)^0,\pm5*\left[(1.005)^0 + (1.005)^1\right],...,\pm5*\left[\sum_{i=0}^{j}(1.005)^i\right]\right\}$$

for integers *k*, *j*, which depend on the propagation distance for the source. For this analysis, *k* = 20,000 and *j* = 600.

With these steps, $f(z_0) = \int_{-\infty}^{\infty}\int_{-\infty}^{\infty} D(m_{\max SPL}(x,y,z_0))dxdy$ is approximated as

$$\sum_{z\in Y}\sum_{x\in X} D(m_{\max SPL}(x,y,z_0))\Delta x \Delta y$$

where *X*,*Y* are defined as above.

This calculation must be repeated for each $z_0 \in Z$, to build the discrete function *f*(*z*).

With the calculation of *f*(*z*) complete, the integral of its product with $\rho(z)$ must be calculated to complete evaluation of

$$\int_{-\infty}^{\infty} \rho(z) \int_{-\infty}^{\infty}\int_{-\infty}^{\infty} D(m_{\max SPL}(x,y,z))dxdydz = \int_{-\infty}^{0} \rho(z) f(z)dz$$

Since *f*(*z*) is discrete, and $\rho(z)$ can be readily made discrete, this equation is approximated numerically as $\sum_{z \in Z} \rho(z) f(z)$, a dot product.

D.5.7 Preserving Calculations for Future Use

Calculating *f*(*z*) is the most time-consuming part of the numerical integration, but the most time-consuming portion of the entire process is calculating $m_{\max SPL}(x,y,z)$ over the area range required for the minimum cutoff value (120 dB). The calculations usually require propagation estimates out to over 100 km, and those estimates, with the beam pattern, are used to construct a sound field that extends 200 km × 200 km = 40,000 sq km, with a calculation at the steps for every value of *X* and *Y*, defined above. This is repeated for each depth, to a maximum of 2,000 meters.

Saving the entire $m_{\max SPL}$ for each *z* is unrealistic, requiring great amounts of time and disk space. Instead, the different levels in the range of $m_{\max SPL}$ are sorted into 0.5 dB wide bins; the volume of water at each bin level is taken from $m_{\max SPL}$, and associated with its bin. Saving this, the amount of water ensonified at each level, at a 0.5 dB resolution, preserves the ensonification information without using the space and time required to save $m_{\max SPL}$ itself. Practically, this is a histogram of occurrence of level at each depth, with 0.5 dB bins. Mathematically, this is simply defining the discrete functions $V_z(L)$, where $L = \{.5a\}$ for every positive integer *a*, and for all $z \in Z$. These functions, or histograms, are saved for future work. The information lost by saving only the histograms is *where* in space the different levels occur, although *how often* they occur is saved. But the thresholds (risk function curves) are purely a function of level, not location, so this information is sufficient to calculate *f*(*z*).

Applying the risk function to the histograms is a dot product:

$$\sum_{\ell \in L_1} D(\ell) V_{z_0}(\ell) \approx \int_{-\infty}^{\infty}\int_{-\infty}^{\infty} D(m_{\max SPL}(x,y,z_0))dxdy$$

So, once the histograms are saved, neither $m_{\max SPL}(x,y,z)$ nor *f*(*z*) must be recalculated to generate $\int_{-\infty}^{0} \rho(z) \int_{-\infty}^{\infty}\int_{-\infty}^{\infty} D(m_{\max SPL}(x,y,z))dxdydz$ for a new threshold function.

For the interested reader, the following section includes an in-depth discussion of the method, software, and other details of the *f*(*z*) calculation.

D.5.8 Software Detail

The risk-function metric uses the aforementioned Feller function to determine the probability that an animal is affected by a given sound pressure level. The acoustic quantity of interest is the maximum sound pressure level (SPL) experienced over multiple pings in a range-independent environment. The procedure for calculating the impact volume at a given depth is relatively simple. In brief, given the SPL of the source and the transmission loss (TL) curve, the received SPL is calculated on a volumetric grid. For a given depth, volume associated with each SPL interval is calculated. Then, this volume is multiplied by the probability that an animal will be affected by that sound pressure level. This gives the impact volume for that depth, which can be multiplied by the animal densities at that depth, to obtain the number of animals affected at that depth. The process repeats for each depth to construct the impact volume as a function of depth.

The case of a single emission of sound energy, one ping, illustrates the computational process in more detail. First, the sound pressure levels are segregated into a sequence of bins that cover the range encountered in the area. The SPL are used to define a volumetric grid of the local sound field. The impact volume for each depth is calculated as follows: for each depth in the volumetric grid, the SPL at each *xy*-plane grid point is calculated using the SPL of the source, the TL curve, the horizontal beam pattern of the source, and the vertical beam patterns of the source. The sound pressure levels in this grid become the bins in the volume histogram.

Figure D-14 shows an example volume histogram for a low-power source. Level bins are 0.5 dB in width and the depth is 50 meters in an environment with water depth of 100 meters. The oscillatory structure at very low levels is due to the flattening of the TL curve at long distances from the source, which magnifies the fluctuations of the TL as a function of range. The “expected” impact volume for a given level at a given depth is calculated by multiplying the volume in each level bin by the risk function evaluated at that level. Total expected impact volume for a given depth is the sum of these “expected” volumes.

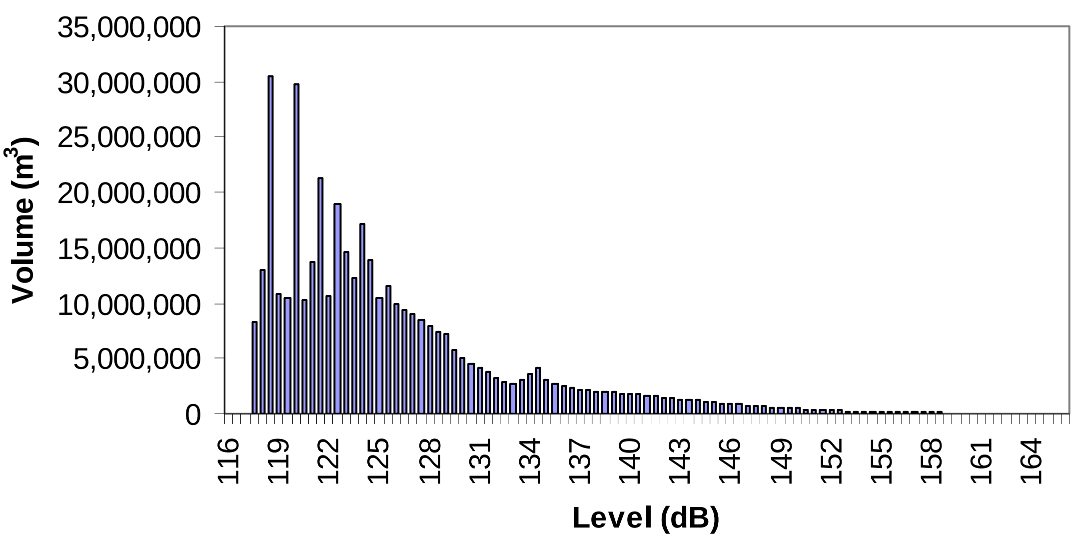

Figure D-14. Example of a Volume Histogram

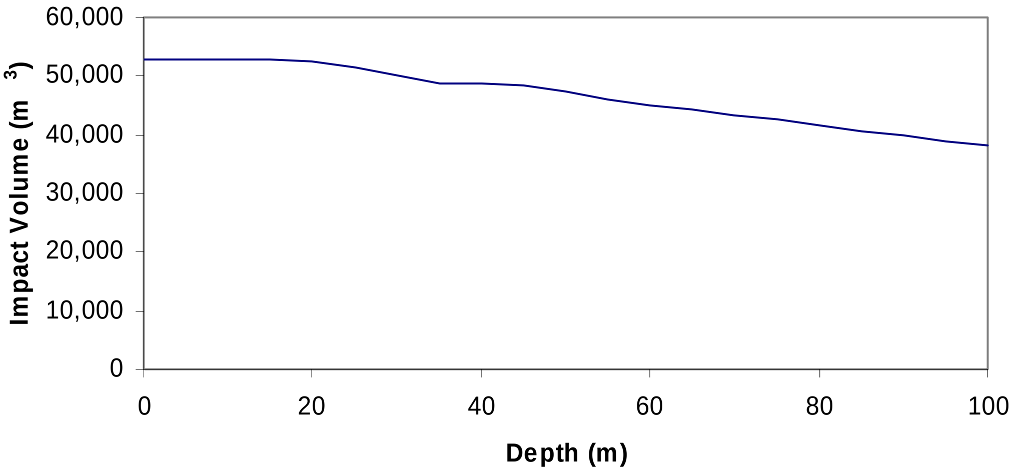

Figure D-15. Example of the Dependence of Impact Volume on Depth

The volumetric grid covers the waters in and around the area of a source's operation. The grid for this analysis has a uniform spacing of 5 meters in the *x*-coordinate and a slowly expanding spacing in the *y*-coordinate that starts with 5 meters spacing at the origin. The growth of the grid size along the *y*-axis is a geometric series where each successive grid size is obtained from the previous by multiplying it by 1 + *Ry*, where *Ry* is the *y*-axis growth factor. The n^{th} grid size is related to the first grid size by multiplying by $(1 + Ry)^{(n-1)}$. For an initial grid size of 5 meters and a growth factor of 0.005, the 100^{th} grid increment is 8.19 meters. The constant spacing in the *x*-coordinate allows greater accuracy as the source moves along the *x*-axis. The slowly increasing spacing in *y* reduces computation time, while maintaining accuracy, by taking advantage of the fact that TL changes more slowly at longer distances from the source. The *x*-and *y*-coordinates extend from $-R_{max}$ to $+R_{max}$, where R_{max} is the maximum range used in the TL calculations. The *z* direction uses a uniform spacing of 5 meters down to 1000 meters and 10 meters from 1000 to 2000 meters. This is the same depth mesh used for the effective energy metric as described above. The depth mesh does not extend below 2000 meters, on the assumption that animals of interest are not found below this depth.

The next three figures indicate how the accuracy of the calculation of impact volume depends on the parameters used to generate the mesh in the horizontal plane. Figure D-16 shows the relative change of impact volume for one ping as a function of the grid size used for the *x*-axis. The *y*-axis grid size is fixed at 5 m and the *y*-axis growth factor is 0, i.e., uniform spacing. The impact volume for a 5 meters grid size is the reference. For grid sizes between 2.5 and 7.5 meters, the change is less than 0.1%. A grid size of 5 meters for the *x*-axis is used in the calculations.

Figure D-17 shows the relative change of impact volume for one ping as a function of the grid size used for the x-axis and the *y*-axis grids, respectively. The *x*-axis grid size is fixed at 5 meters and the *y*-axis growth factor is 0. The impact volume for a 5 meters grid size is the reference. This figure is very similar to that for the *x*-axis grid size. For grid sizes between 2.5 and 7.5 meters, the change is less than 0.1%. A grid size of 5 meters is used for the *y*-axis in our calculations. Figure D-18 shows the relative change of impact volume for one ping as a function of the *y*-axis growth factor. The *x*-axis grid size is fixed at 5 meters and the initial *y*-axis grid size is 5 meters. The impact volume for a growth factor of 0 is the reference. For growth factors from 0 to 0.01, the change is less than 0.1%. A growth factor of 0.005 is used in the calculations.

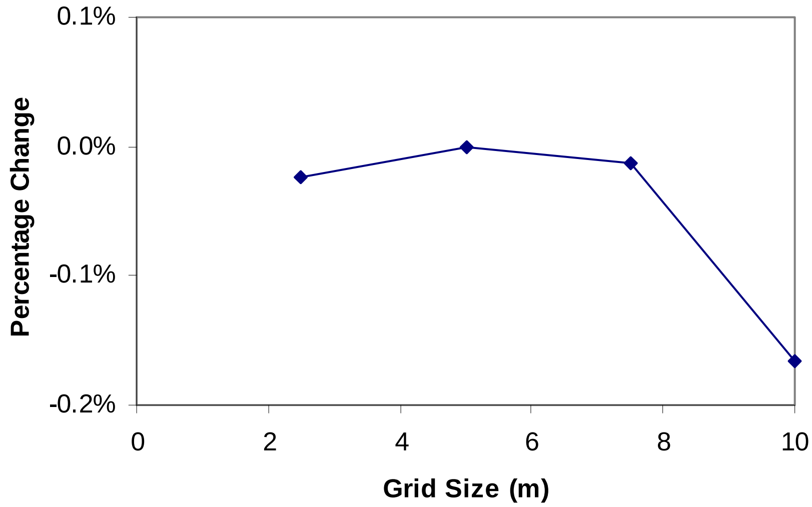

Figure D-16. Change of Impact Volume as a Function of *x*-axis Grid Size

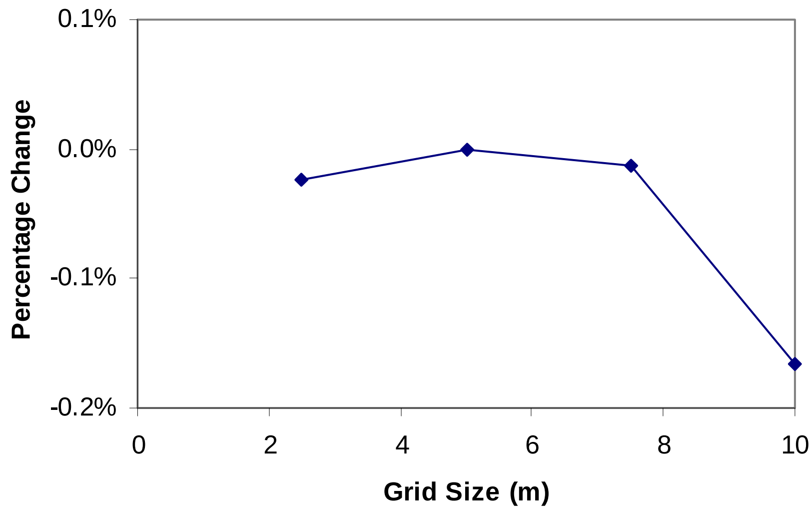

Figure D-17. Change of Impact Volume as a Function of y-axis Grid Size

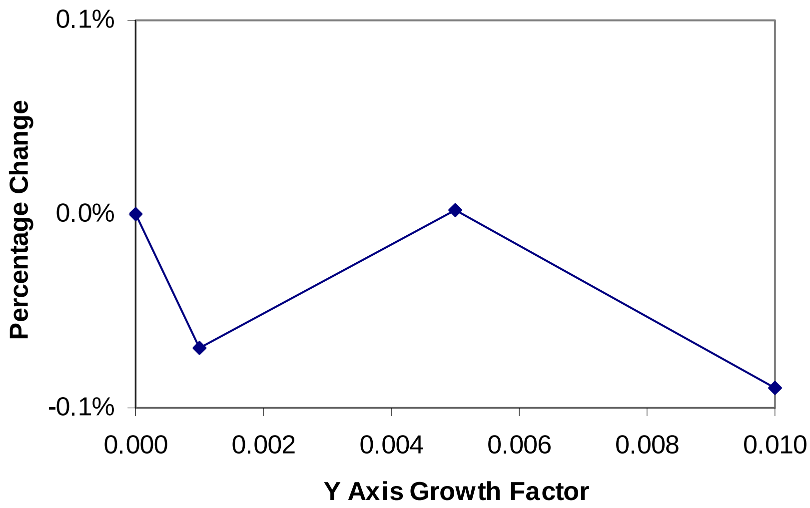

Figure D-18. Change of Impact Volume as a Function of y-axis Growth Factor

Another factor influencing the accuracy of the calculation of impact volumes is the size of the bins used for sound pressure level. The sound pressure level bins extend from 100 dB (far lower than required) up to 300 dB (much higher than that expected for any sonar system).

Figure D-19 shows the relative change of impact volume for one ping as a function of the bin width. The *x*-axis grid size is fixed at 5 meters, and the initial *y*-axis grid size is 5 meters with a *y*-axis growth factor of 0.005. The impact volume for a bin size of 0.5 dB is the reference. For bin widths from 0.25 dB to 1.00 dB, the change is about 0.1%. A bin width of 0.5 is used in our calculations.

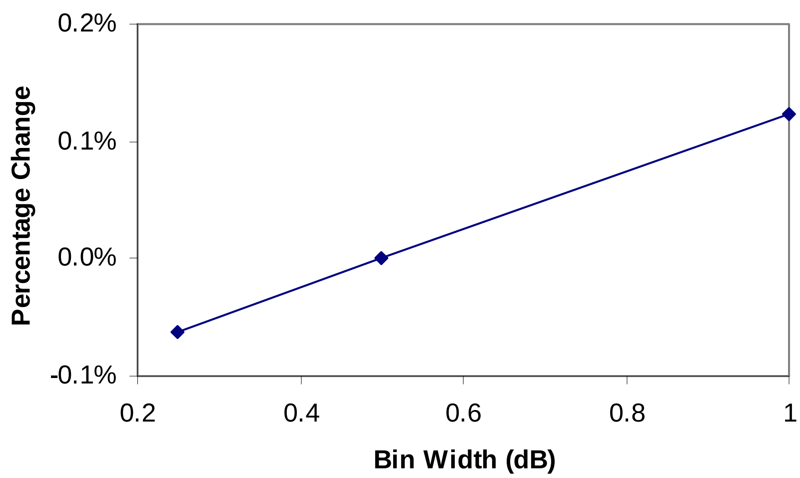

Figure D-19. Change of Impact Volume as a Function of Bin Width

Two other issues for discussion are the maximum range (R_{max}) and the spacing in range and depth used for calculating TL. The TL generated for the energy accumulation metric is used for dose-response analysis. The same sampling in range and depth is adequate for this metric because it requires a less demanding computation (i.e., maximum value instead of accumulated energy). Using the same value of R_{max} needs some discussion since it is not clear that the same value can be used for both metrics. R_{max} was set so that the TL at R_{max} is more than needed to reach the energy accumulation threshold of 173 dB for 1000 pings. Since energy is accumulated, the same TL can be used for one ping with the source level increased by 30 dB (10 $\log_{10}$(1000)). Reducing the source level by 30 dB, to get back to its original value, permits the handling of a sound pressure level threshold down to 143 dB, comparable to the minimum required. Hence, the TL calculated to support energy accumulation for 1000 pings will also support calculation of impact volumes for the dose-response metric.

The process of obtaining the maximum sound pressure level at each grid point in the volumetric grid is straightforward. The active sonar starts at the origin and moves at constant speed along the positive x-axis emitting a burst of energy, a ping, at regularly spaced intervals. For each ping, the distance and horizontal angle connecting the source to each grid point is computed. Calculating the TL from the source to a grid point has several steps. The TL is made up of the sum of many eigenrays connecting the source to the grid point. The beam pattern of the source is applied to the eigenrays based on the angle at which they leave the source. After summing the vertically beamformed eigenrays on the range mesh used for the TL calculation, the vertically beamformed TL for the distance from the sonar to the grid point is derived by interpolation. Next, the horizontal beam pattern of the source is applied using the horizontal angle connecting the sonar to the grid point. To avoid problems in extrapolating TL, only grid points with distances less than R_{max} are used. To obtain the sound pressure level at a grid point, the sound pressure level of the source is reduced by that TL. For the first ping, the volumetric grid is populated by the calculated sound pressure level at each grid point. For the second ping and subsequent pings, the source location increments along the x-axis by the spacing between pings and the sound pressure level for each grid point is again calculated for the new source location. Since the risk-function metric uses the maximum of the sound pressure levels at each grid point, the newly calculated sound pressure level at each grid point is compared to the sound pressure level stored in the grid. If the new level is larger than the stored level, the value at that grid point is replaced by the new sound pressure level.

For each bin, a volume is determined by summing the ensonified volumes with a maximum SPL in the bin's interval. This forms the volume histogram shown in Figure D-14. Multiplying by the dose-response probability function for the level at the center of a bin gives the impact volume for that bin. The result can be seen in Figure D-15, which is an example of the impact volume as a function of depth.

The impact volume for a sonar moving relative to the animal population increases with each additional ping. The rate at which the impact volume increases for the risk function metric is essentially linear with the number of pings. Figure D-20 shows the dependence of impact volume on the number of pings. The slope of the line at a given depth is the impact volume added per ping. This number multiplied by the number of pings in an hour gives the hourly impact volume for the given depth increment. Completing this calculation for all depths in a province, for a given source, gives the hourly impact volume vector which contains the hourly impact volumes by depth for a province.

Figure D-21 provides an example of an hourly impact volume vector for a particular environment. Given the speed of the sonar platform, the hourly impact volume vector could be displayed as the impact volume vector per kilometer of track.

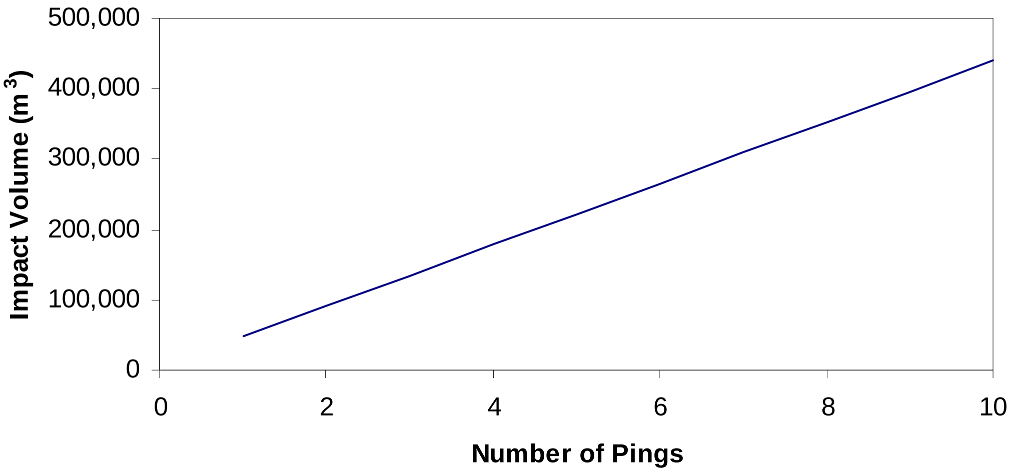

Figure D-20. Dependence of Impact Volume on the Number of Pings

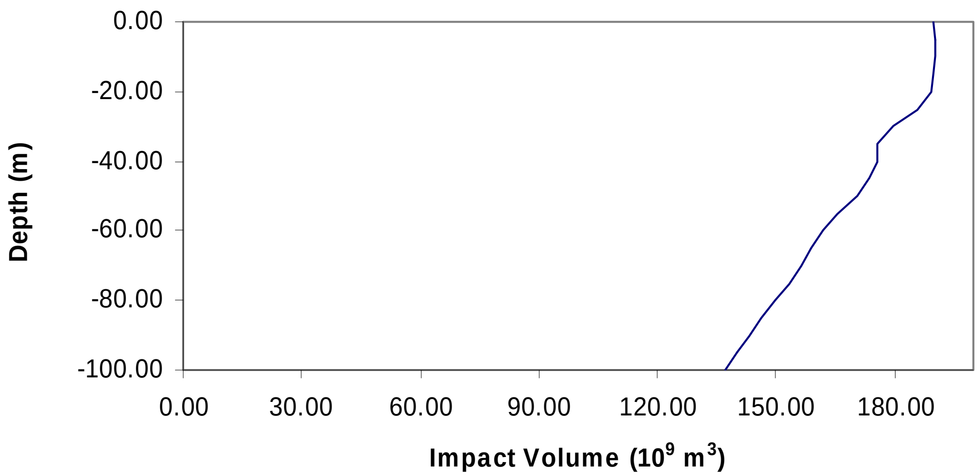

Figure D-21. Example of an Hourly Impact Volume Vector

D.5.9 Modeling Quiet and Continuous Sources

The TMAA has modeled sources whose energy contributions do not exceed EFDL thresholds, but have source levels above 120 dB, and move in a continuous fashion. The previous discussion of software detail would present under-sampling artifacts when applied to quiet sources, so an alternative approach is implemented.

Consider transmission loss with cylindrical symmetry surrounding an omni-directional source (Figure D-22):

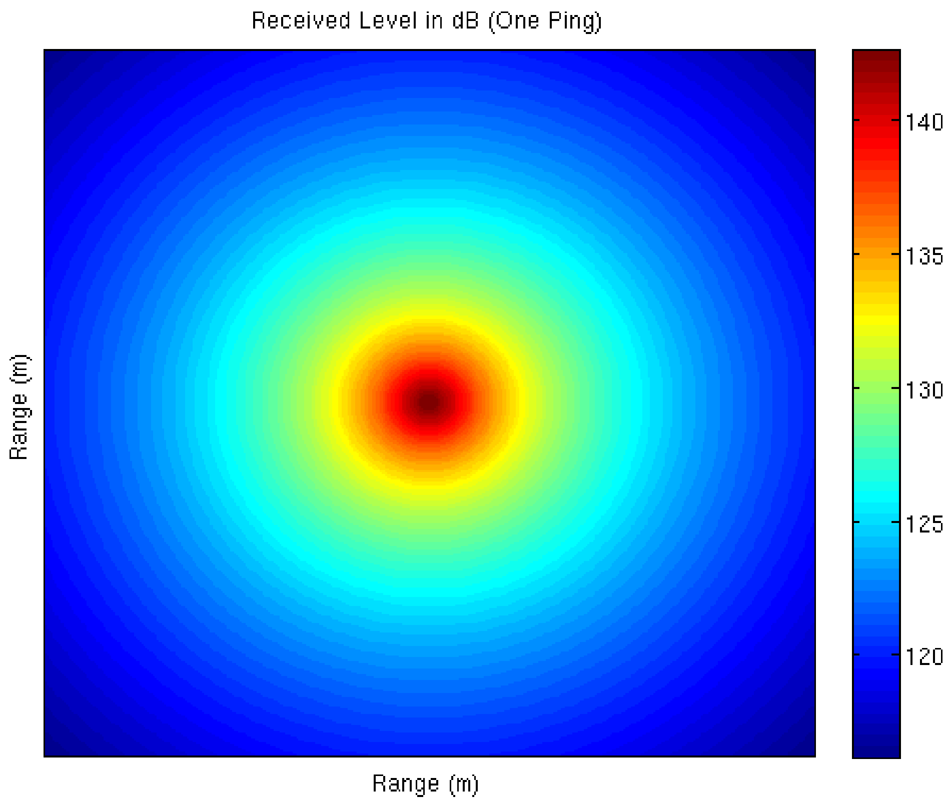

Figure D-22. – Single Ping Maximum SPL Field

When the factors of continuous pinging behavior, monotonic transmission loss in the short range, and maximum SPL as the input metric for the risk function, computing the maximum SPL field is a matter of extending the field as such (Figure D-23):

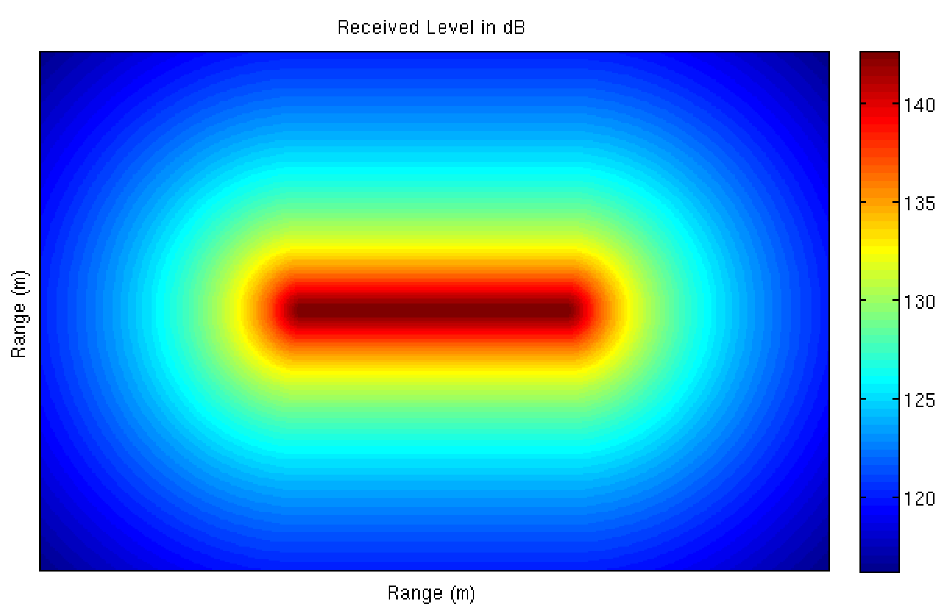

Figure D-23. – Quiet Continuous Sound Source

In the direction orthogonal to source motion, maximum SPL is achieved at CPA. This algorithm takes a 0.5-meter resolution frequency-dependent TL curve and proceeds as follows.

In a given depth interval:

- Find the received level in one meter increments about a source. In the first one meter step, calculate the area of circle ensonified at the matching received level.
- Calculate areas of subsequent n^{th} circles in 1 meter steps.
- Compute the area on a rectangular strip for a one-meter extent in parallel to annulus radius of equivalent received level. Scale by the probability of harassment based on received level at this n^{th} range. Note that received level at the outer-radius of the modified annulus was used to calculate the probability with the risk function.
- Convert annulus result to volume based on the depth increment.
- Sum all scaled volumes of interior cylinder and subsequent annuli to impact range at 120 dB to find a cumulative volume for this depth interval which inherits the probabilistic calculation.

This algorithm takes place over the entire water column to capture dynamics of ensonification over all depths, and hence produces an impact volume vector.

D.6 HARRASSMENTS

This section defines the animal densities and their depth distributions for the TMAA. This is followed by a series of tables providing MMPA harassment estimates per unit of operation for each source type (active sound sources and explosives).

D.6.1 Animal Densities

Densities are usually reported by marine biologists as animals per square kilometer, which is an area metric. This gives an estimate of the number of animals below the surface in a certain area, but does not provide any information about their distribution in depth. The impact volume vector (see subsection D.4.3) specifies the volume of water ensonified above the specified threshold in each depth interval. A corresponding animal density for each of those depth intervals is required to compute the expected value of the number of exposures. The two-dimensional area densities do not contain this information, so three-dimensional densities must be constructed by using animal depth distributions to extrapolate the density at each depth. The required depth distributions are presented in the biology subsection.

D.6.2 Harassment Estimates

The following sperm whale example demonstrates the methodology used to create a three-dimensional density by merging the area densities with the depth distributions. The sperm whale surface density is 0.0003 whales per square kilometer. From the depth distribution report, "depth distribution for sperm whales based on information in the Amano paper is: 31% in 0-10 m, 8% in 10-200 m, 9% in 201-400 m, 9% in 401-600 m, 9% in 601-800 m and 34% in >800 m." So the sperm whale density at 0-10 m is 0.0003*0.31/0.01 = 0.0093 per cubic km, at 10-200 m is 0.0003*0.08/0.19 = .00012632 per cubic km, and so forth.

In general, the impact volume vector samples depth in finer detail than given by the depth distribution data. When this is the case, the densities are apportioned uniformly over the appropriate intervals. For example, suppose the impact volume vector provides volumes for the intervals 0-10 meters, 10-50 meters, and 50-200 meters. Then for the depth-distributed densities discussed in the preceding paragraph,

- 0.0093 whales per cubic km is used for 0-10 meters,
- 0.00012632 whales per cubic km is used for the 10-50 meters, and
- 0.00012632 whales per cubic km is used for the 50-200 meters.

Once depth-varying, three-dimensional densities are specified for each species type, with the same depth intervals and the ensonified volume vector, the density calculations are finished. The expected number of ensonified animals within each depth interval is the ensonified volume at that interval multiplied by the volume density at that interval and this can be obtained as the dot product of the ensonified volume and animal density vectors.

Since the ensonified volume vector is the ensonified volume per unit operation (i.e. per hour, per sonobuoy, etc), the final harassment count for each animal is the unit operation harassment count multiplied by the number of units (hours, sonobuoys, etc).

D.6.3 Additional Modeling Considerations in a General Modeling Scenario

When modeling the effect of sound projectors in the water, the ideal task presents modelers with complete *a priori* knowledge of the location of the source(s) and transmission patterns during the times of interest. In these cases, calculation inputs include the details of source path, proximity of shoreline, high-resolution density estimates, and other details of the scenario. However, in the TMAA, there are sound-producing events for which the source locations and transmission patterns are unknown, but still require analysis to predict effects. For these cases, a more general modeling approach is required: “We will be operating somewhere in this large area for *X* minutes. What are the potential effects on average?”

Modeling these general scenarios requires a statistical approach to incorporate the scenario nuances into harassment calculations. For example, one may ask: “If an animal receives 130 dB SPL when the source passes at closest point of approach (CPA) on Tuesday morning, how do we know it doesn't receive a higher level on Tuesday afternoon?” This question cannot be answered without knowing the path of the source (and several other facts). Because the path of the source is unknown, the number of an individual's re-exposures cannot be calculated directly. But it can, on average, be accounted for by making appropriate assumptions.

Table D-14 lists unknowns created by uncertainty about the specifics of a future proposed action, the portion of the calculation to which they are relevant, and the assumption that allows the effect to be computed without the detailed information:

Table D-14 – Unknowns and Assumptions

Unknowns	Relevance	Assumption
Path of source (esp. with respect to animals)	Ambiguity of multiple exposures, Local population: upper bound of harassments	Most conservative case: sources can be anywhere within range
Source locations	Ambiguity of multiple exposures, land shadow	Equal distribution of action in each range
Direction of sonar transmission	Land shadow	Equal probability of pointing any direction

The following sections discuss two topics that require action details, and describe how the modeling calculations used the general knowledge and assumptions to overcome the future-action uncertainty with respect to re-exposure of animals, and land shadow.

D.6.4 Multiple Exposures in General Modeling Scenario

Consider the following hypothetical scenario. A box is painted on the surface of a well-studied ocean environment with well-known propagation. A sound source and 100 whales are inserted into that box and a curtain is drawn. What will happen? The details of what will happen behind the curtain are unknown, but the existing knowledge, and general assumptions, can allow for a calculation of average affects.

For the first period of time, the source is traveling in a straight line and pinging at a given rate. In this time, it is known how many animals, on average, receive their max SPLs from each ping. As long as the source travels in a straight line, this calculation is valid. However, after an undetermined amount of time, the source will change course to a new and unknown heading.

If the source changes direction 180 degrees and travels back through the same swath of water, all the animals the source passes at closest point of approach (CPA) before the next course change have already been exposed to what will be their maximum SPL, so the population is not "fresh." If the direction does not change, only new animals will receive what will be their maximum SPL from that source (though most have received sound from it), so the population is completely "fresh." Most source headings lead to a population of a mixed "freshness," varying by course direction. Since the route and position of the source over time are unknown, the freshness of the population at CPA with the source is unknown. This ambiguity continues through the remainder of the exercise.

What is known? The source and, in general, the animals remain in the vicinity of the range. Thus, if the farthest range to a possible effect from the source is *X* km, no animals farther than *X* km outside of the TMAA can be harassed. The intersection of this area with a given animal's habitat multiplied by the density of that animal in its habitat represents the maximum number of animals that can be harassed by activity in that TMAA, which shall be defined as "the local population." Two details: first, this maximum should be adjusted down if a risk function is being used, because not 100% of animals within *X* km of the TMAA border will be harassed. Second, it should be adjusted up to account for animal motion in and out of the area.

The ambiguity of population freshness throughout the exercise means that multiple exposures cannot be calculated for any individual animal. It must be dealt with generally at the population level.

D.6.4.1 Solution to the Ambiguity of Multiple Exposures in the General Modeling Scenario

At any given time, each member of the population has received a maximum SPL (possibly zero) that indicates the probability of harassment in the exercise. This probability indicates the contribution of that individual to the expected value of the number of harassments. For example, if an animal receives a level that indicates 50% probability of harassment, it contributes 0.5 to the sum of the expected number of harassments. If it is passed later with a higher level that indicates a 70% chance of harassment, its contribution increases to 0.7. If two animals receive a level that indicates 50% probability of harassment, they together contribute 1 to the sum of the expected number of harassments. That is, we statistically expect exactly one of them to be harassed. Let the expected value of harassments at a given time be defined as "the harassed population" and the difference between the local population (as defined above) and the harassed population be defined as "the unharassed population." As the exercise progresses, the harassed population will never decrease and the unharassed population will never increase.

The unharassed population represents the number of animals statistically "available" for harassment. Since we do not know where the source is, or where these animals are, we assume an average (uniform) distribution of the unharassed population over the area of interest. The densities of unharassed animals are lower than the total population density because some animals in the local population are in the harassed population.

Density relates linearly to expected harassments. If action A in an area with a density of 2 animals per square kilometer produces 100 expected harassments, then action A in an area with 1 animal per square kilometer produces 50 expected harassments. The modeling produces the number of expected harassments per ping starting with 100% of the population unharassed. The next ping will produce slightly fewer harassments because the pool of unharassed animals is slightly less.

For example, consider the case where 1 animal is harassed per ping when the local population is 100, 100% of which are initially unharassed. After the first ping, 99 animals are unharassed, so the number of animals harassed during the second ping are

$$1\left(\frac{99}{100}\right) = 1(.99) = 0.99 \text{ animals}$$

and so on for the subsequent pings.

Mathematics

A closed form function for this process can be derived as follows.

Define $H =$ number of animals harassed per ping with 100% unharassed population. H is calculated by determining the expected harassments for a source moving in a straight line for the duration of the exercise and dividing by the number of pings in the exercise (Figure D-24).

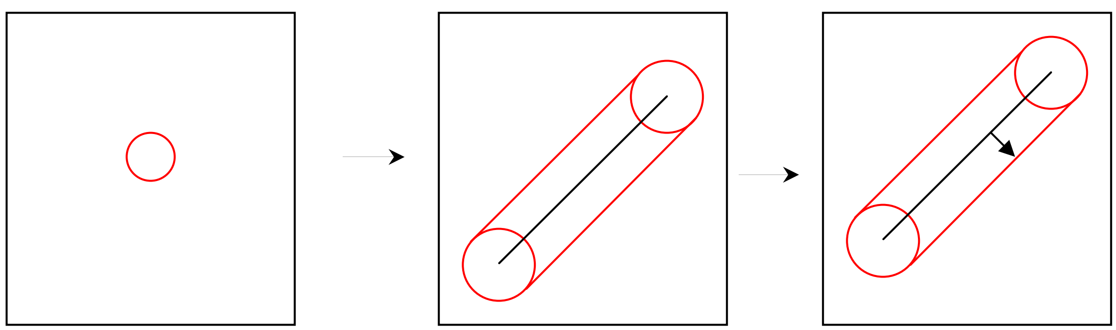

Figure D-24. – Process of calculating *H*

$$H = \frac{\iiint \rho(z) D(L(x,y,z))dxdydz}{N_{pings}}$$

The total un-harassed population is then calculated by iteration. Each ping affects the un-harassed population left after all previous pings:

Define $P_n =$ unharassed population after n^{th} ping

$$P_0 = \text{local population}$$

$$P_1 = P_0 - H$$
$$P_2 = P_1 - H\left(\frac{P_1}{P_0}\right)$$
$$\ldots$$
$$P_n = P_{n-1} - H\left(\frac{P_{n-1}}{P_0}\right)$$

Therefore,

$$P_n = P_{n-1}\left(1-\left(\frac{H}{P_0}\right)\right) = P_{n-2}\left(1-\left(\frac{H}{P_0}\right)\right)^2 = \ldots = P_0\left(1-\left(\frac{H}{P_0}\right)\right)^n$$

Thus, the total number of harassments depends on the per-ping harassment rate in an un-harassed population, the local population size, and the number of operation hours.

D.6.4.2 Local Population: Upper Bound on Harassments

As discussed above, Navy planners have confined periods of sonar use to operation areas. The size of the harassed population of animals for an action depends on animal re-exposure, so uncertainty about the precise source path creates variability in the "harassable" population. Confinement of sonar use to a sonar operating area allows modelers to compute an upper bound, or worst case, for the number of harassments with respect to location uncertainty. This is done by assuming that every animal which enters the operation area at any time in the exercise (and also many outside) is "harassable" and creates an upper bound on the number of harassments for the exercise. Since this is equivalent to assuming that there are sonars transmitting simultaneously from each point in the confined area throughout the action length, this greatly overestimates the harassments from an exercise.

NMFS has defined a twenty-four hour "refresh rate," or amount of time in which an individual animal can be harassed no more than once. The Navy has determined that, in a twenty-four hour period, all training events in the TMAA involve sources that transmit for no longer than sixteen (16) hours.

The most conservative assumption for a single ping is that it harasses the entire population within the range (a gross over-estimate). However, the total harassable population for multiple pings will be even greater since animal motion over the period in the above table can bring animals into range that otherwise would be out of the harassable population.

D.6.4.3 Animal Motion Expansion

Though animals often change course to swim in different directions, straight-line animal motion would bring the more animals into the harassment area than a "random walk" motion model. Since precise and accurate animal motion models exist more as speculation than documented fact and because the modeling requires an undisputable upper bound, calculation of the upper bound for TMAA modeling areas uses a straight-line animal motion assumption. This is a conservative assumption.

For a circular area, the straight-line motion in any direction produces the same increase in harassable population. However, since the ranges are non-circular polygons, choosing the initial fixed direction as perpendicular to the longest diagonal produces greater results than any other direction. Thus, the product of the longest diagonal and the distance the animals move in the period of interest gives an overestimate of the expansion in range modeling areas due to animal motion. The expansions use this estimate as an absolute upper bound on animal-motion expansion.

Figure D-25 illustrates the overestimation, which occurs during the second arrow:

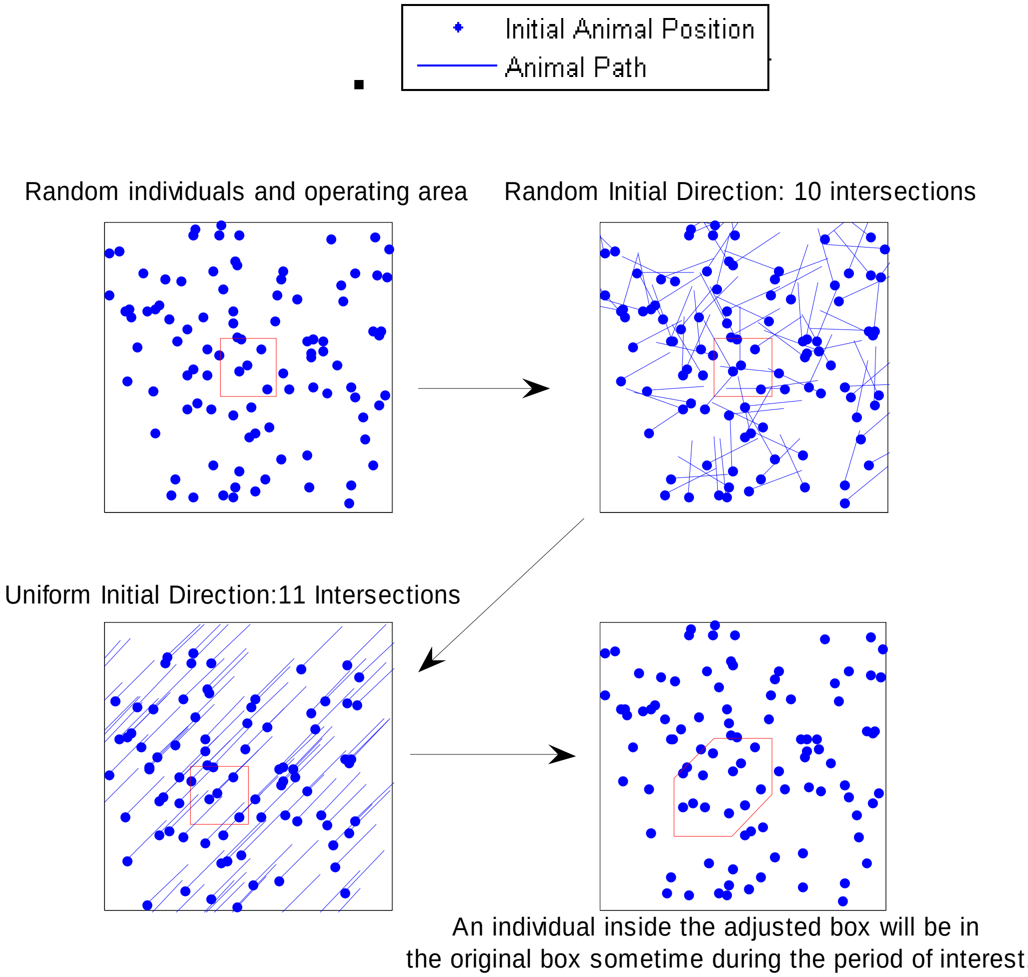

Figure D-25. Process of Setting an Upper Bound on Individuals Present in Area

It is important to recognize that the area used to calculate the harassable population, shown in Figure D-25 will, in general, be much larger than the area that will be within the ZOI of a ship for the duration of its broadcasts. For a ship moving faster than the speed of the marine animals, a better (and much smaller) estimate of the harassable population would be that within the straight line ZOI cylinder shown in Figure D-26. Using this smaller population would lead to a greater dilution of the unharassed population per ping and would greatly reduce the estimated harassments.

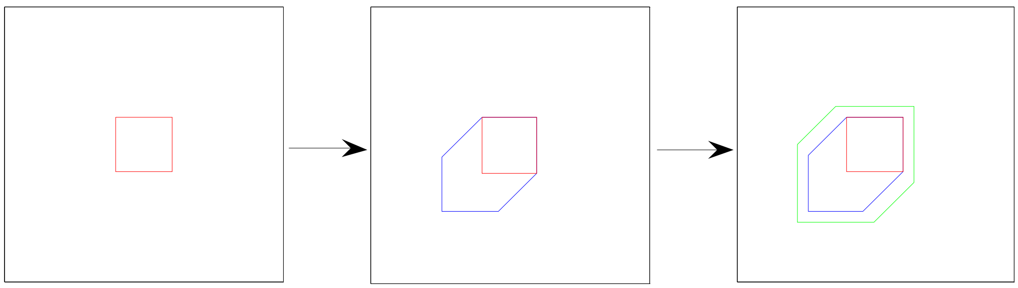

Figure D-26. Process of Expanding Area to Create Upper Bound of Harassments

D.6.4.4 Risk Function Expansion

The expanded area contains the number of animals that will enter the range over the period of interest. However, an upper bound on harassments must also include animals outside the area that would be affected by a source transmitting from the area's edge. A gross overestimation could simply assume pinging at every point on the range border throughout the exercise and would include all area with levels from a source on the closest border point greater than the risk function basement. In the case of GOA, this would include all area within approximately 105 km from the edge of the adjusted box. (See Table D-15). This basic method would give a crude and exaggerated upper bound, since only a tiny fraction of this out-of-range area can be ensonified above threshold for a given ping. A more refined upper bound on harassments can be found by maintaining the assumption that a source is transmitting from each point in the adjusted box and calculating the expected ensonified area, which would give all animals inside the area a 100% probability of harassment, and those outside the area a varying probability, based on the risk function.

$$\int_{0}^{L^{-1}(120\,dB)} D(L(r))dr\,,$$

Where L is the SPL function with domain in range and range in level,

r is the range from the sonar operating area,

L^{-1}(120 dB) is the range at which the received level drops to 120 dB, and

D is the risk function (probability of harassment vs. Level).

At the corners of the polygon, additional area can be expressed as

$$\frac{[\pi-\theta]\displaystyle\int_{0}^{L^{-1}(120\,dB)} D(L(r))rdr}{2\pi}$$

with D, L, and r as above, and

θ the inner angle of the polygon corner, in radians.

For the risk function and transmission loss of the TMAA, this method adds an area equivalent by expanding the boundaries of the adjusted box by four kilometers. The resulting shape, the adjusted box with a boundary expansion of 4 km, does not possess special meaning for the problem. But the number of individuals contained by that shape, is the harassable population and an absolute upper bound on possible harassments for that operation.

The following plots illustrate the growth of area for the sample case above. The shapes of the boxes are unimportant. The area after the final expansion, though, gives an upper bound on the “harassable”, or initially unharassed population which could be affected by operations.

Example Case

Consider a sample case from the TMAA. For the most powerful source, the SQS-53, the expected winter rate of exposures under the risk function considered behaviorial MMPA Level B harassment for minke whales is approximately 0.068985832 harassments per ping. The exercise will transmit sonar pings for 16 hours in a 24 hour period as consistent with planned use, with 120 pings per minute, a total of 120 * 16 = 1,920 pings in a 24 hour period.

The TMAA has an area of approximately 92,246 square kilometers and a diagonal of 486.5 km. Adjusting this with straight-line (upper bound) animal motion of 5.5 kilometers per hour for 16 hours, animal motion adds 486.5 * 5.5 * 16 = 42,812 square kilometers to the area. Using the risk function to calculate the expected range outside the OA approximately adds another 5,068 square kilometers, bringing the total upper-bound of the affected area to 140,126 square km.

For example, minke whales have an average winter density of 0.0006 animals per square kilometer, so the upper bound number of minke whales that can be affected by SQS-53 activity in the GOA during a 24 hour period is 140,126 * 0.0006 = 84.0756 whales.

In the first ping, 0.068985832 minke whales will be harassed. With the second ping,

$0.068985832 \left(\frac{84.0756 - 0.068985832}{84.0756} \right) = 0.068929228$ minke whales will be harassed. Using the formula derived above, after 16 hours of continuous operation, the remaining **unharassed** population is

$$P_{1920} = P_0 \left(1 - \left(\frac{h}{P_0} \right) \right)^{1920} = 84.0756 \left(1 - \left(\frac{0.068985832}{84.0756} \right) \right)^{1920} \approx 17.3861$$

So the **harassed** population will be 84.0756 – 17.3861 = 66.6895 animals.

Contrast this with linear accumulation of harassments without consideration of the local population and the dilution of the unharassed population:

Harassments = 0.068985832 * 1920 = 132.45 whales,

which is 57% greater than the estimated local population of 84.0756 minke whales. Because linear accumulation assumes an infinite local population, it always overestimates the number of harassments, sometimes to the point of producing impossible results.

D.6.5 Land Shadow

The risk function considers the possibility of harassment possible if an animal receives 120 dB sound pressure level, or above. In the open ocean of the GOA, this can occur as far away as 105 km, so over a large "effect" area, sonar sound could, but does not necessarily, harass an animal. The harassment calculations for a general modeling case must assume that this effect area covers only water fully populated with animals, but in some portions of the GOA, land partially encroaches on the area, obstructing sound propagation.

As discussed in the introduction of "Additional Modeling Considerations" Navy planners do not know the exact location and transmission direction of the sonars at future times. These factors however, completely determine the interference of the land with the sound, or "land shadow," so a general modeling approach does not have enough information to compute the land shadow effects directly. However, modelers can predict the reduction in harassments at any point due to land shadow for different pointing directions and use expected probability distribution of activity to calculate the average land shadow for operations in each range.

For each of the coastal points that are within 105 km of the grid, the azimuth and distance are computed. In the computation, only the minimum range at each azimuth is computed.

Now, the average of the distances to shore, along with the angular profile of land is computed (by summing the unique azimuths that intersect the coast) for each grid point. The values are then used to compute the land shadow for the grid points.

D.6.5.1 Computing the Land Shadow Effect at Each Grid Point

The effect of land shadow is computed by determining the levels, and thus the distances from the sources, that the harassments occur. The levels vary according to acoustic propagation conditions, so the analysis breaks down according to two seasons. Table D-15 gives a mathematical extrapolation of the distances and levels at which harassments occur, with average seasonal propagation in the GOA using the SQS-53 as an example and as displayed in Figures D-27 and D-28.

Table D-15 – Behavioral Harassments at each Received Level Band from SQS-53 During Summer Months

Received Level (dB SPL)	Distance at which Levels Occur in GOA	Percent of Behavioral Harassments Occurring at Given Levels
Below 138	42 km – 105 km	~ 0 %
138<Level<144	28 km – 42 km	< 1 %
144<Level<150	17 km – 28 km	~1 %
150<Level<156	9 km – 17 km	7 %
156<Level<162	5 km – 9 km	18 %
162<Level<168	2.5 km – 5 km	26 %
168<Level<174	1.2 km – 2.5 km	22 %
174<Level<180	0.5 km – 1.2 km	14 %
180<Level<186	335 m – 0.5 km	6 %
186<Level<TTS	178 m – 335 m	5 %

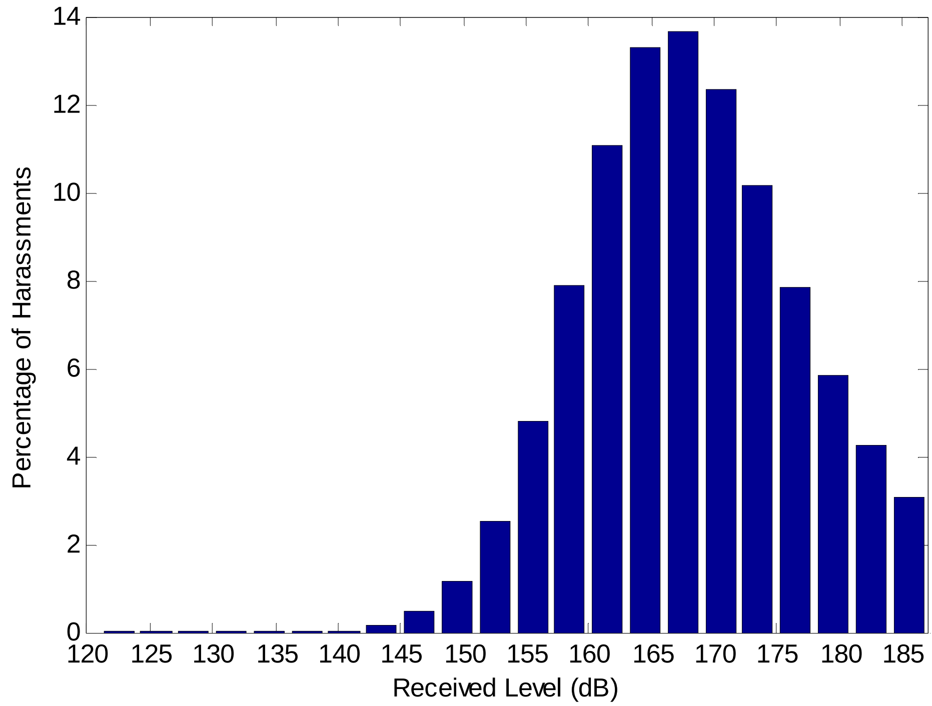

Figure D-27. – The Approximate Percentage of Behavioral Harassments for Every 3 Degree Band of Received Level from the SQS-53 During Summer Months

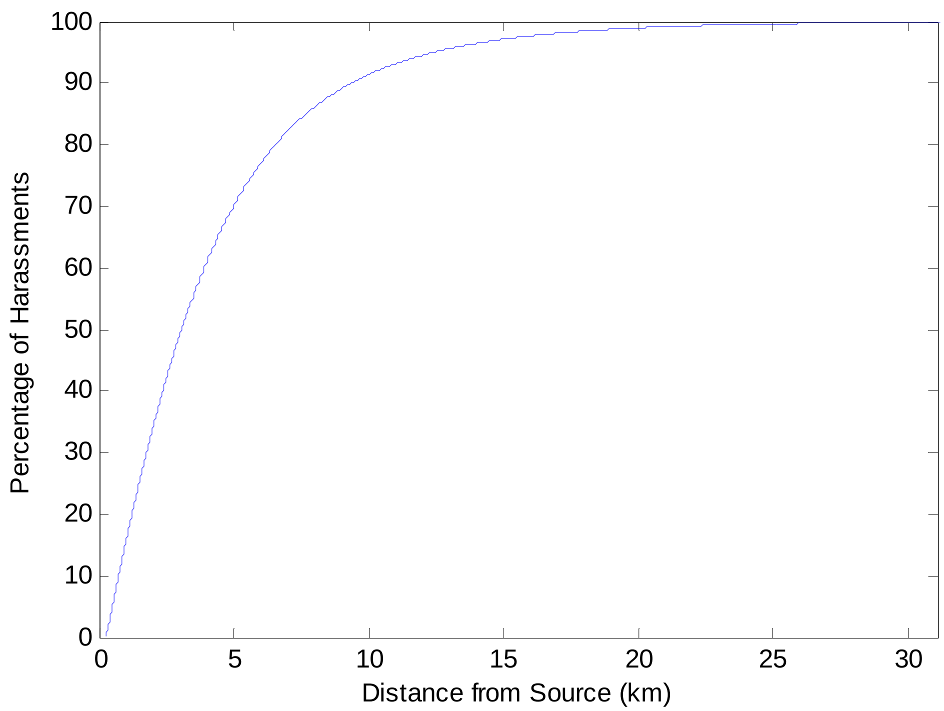

Figure D-28. – Average Percentage of Harassments Occurring Within a Given Distance during Summer Months

With the data used to produce the previous figure, the average effect reduction during summer months for a sound path blocked by land can be calculated. For the SQS-53, since approximately 92% of harassments occur within 10 km of the source, a sound path blocked by land at 10 km will, on average, cause approximately 92% of the effect of an unblocked path.

As described above, the mapping process determines the angular profile of and distance to the coastline(s) from each grid point. The distance, then, determines the reduction due to land shadow when the sonar is pointed in that direction. The angular profile, then, determines the probability that the sonar is pointed at the coast.

Define θ_n = angular profile of coastline at point n in radians

Define r_n = mean distance to shoreline

Define $A(r)$ = average effect adjustment factor for sound blocked at distance r

The land shadow at point n can be approximated by $A(r_n)\theta_n/(2\pi)$. For illustration, the following plot gives the land shadow reduction factor at each point in each range area for the SQS-53 (Figure D-29) . The white portions of the plot indicate the areas outside the range and the blue lines indicate the coastline. The color plots inside the ranges give the land shadow factor at each point. The average land shadow factor for the SQS-53 in the GOA is essentially 1, or the reduction in effect is 0% for both seasons. For the other, lower-power sources it follows that this reduction is also negligible.

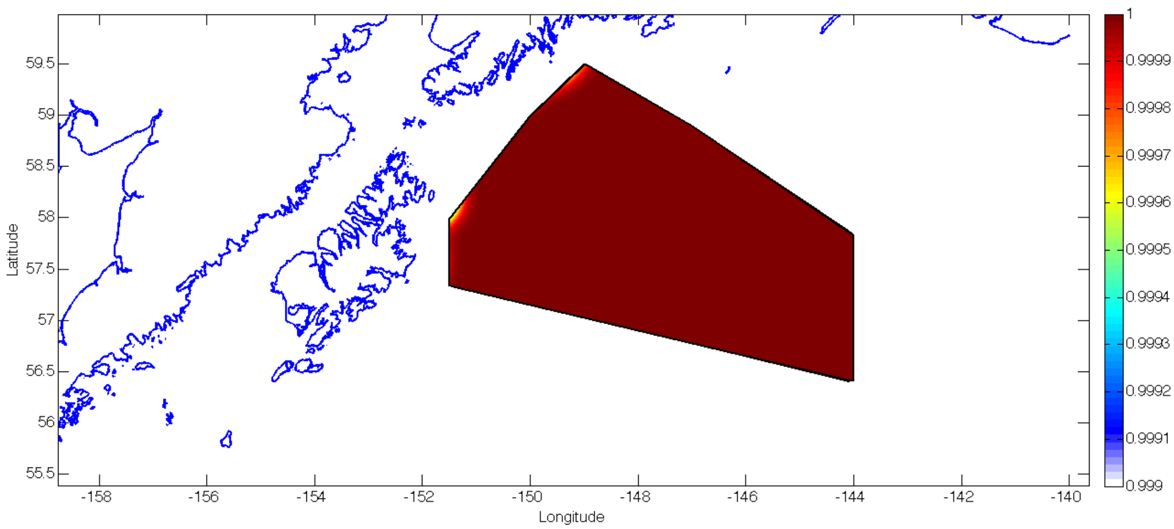

Figure D-29. – Depiction of Land Shadow over the TMAA

D.6.5.2 The Effect of Multiple Ships

Behavioral harassment, under dose response (risk function), uses maximum sound pressure level over a 24 hour period as the metric for determining the probability of harassment. An animal that receives sound from two sonars, operating simultaneously, receives its maximum sound pressure level from one of the ships. Thus, the effects of the louder, or closer, sonar determine the probability of harassment, and the more distant sonar does not. If the distant sonar operated by itself, it would create a lesser effect on the animal, but in the presence of a more dominating sound, its effects are cancelled. When two sources are sufficiently close together, their sound fields within the cutoff range will partially overlap and the larger of the two sound fields at each point in that overlap cancel the weaker. If the distance between sources is twice as large as the range to cutoff, there will be no overlap.

Computation of the overlap between sound fields requires the precise locations and number of the source ships. The general modeling scenarios of the TMAA do not have these parameters, so the effect was modeled using an average ship distance, 20 km, and an average number of ships per exercise, in this case three ships.

The formation of ships in any of the above exercised has been determined by Navy planners. The ships are located in a straight line, perpendicular to the direction has traveled. The figures below (D-30 to D-34) show examples with four ships, and their ship tracks.

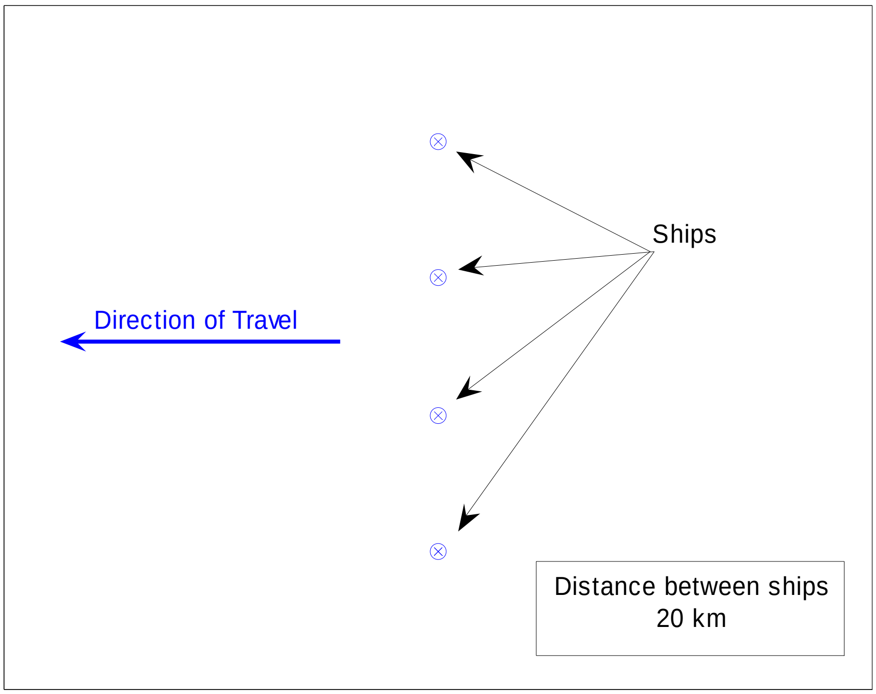

Figure D-30. – Formation and Bearing of Ships in 4-Ship Example

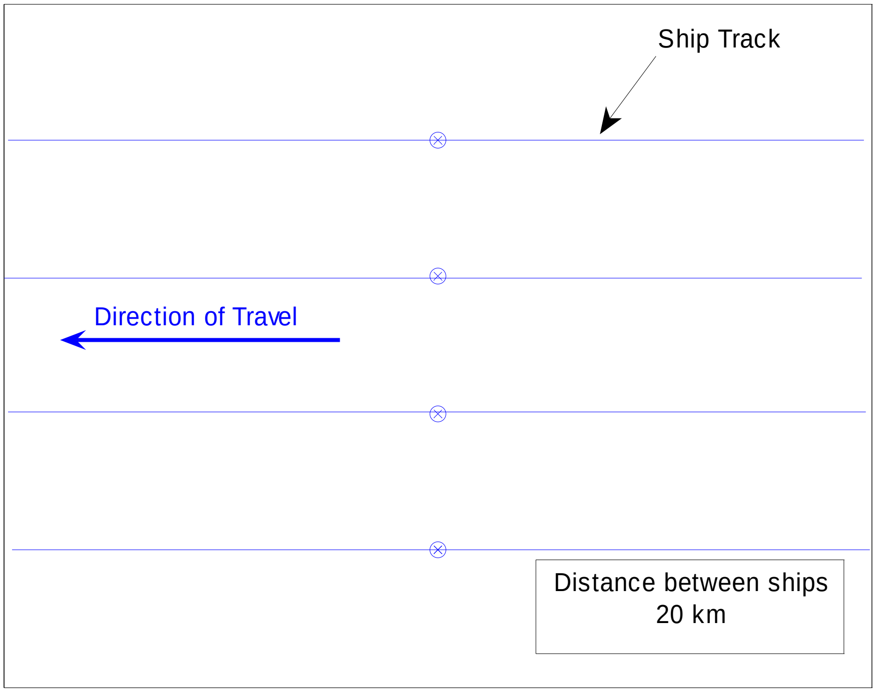

Figure D-31. – Ship Tracks of Ships in 4-Ship Example

The sound field created by these ships, which transmit sonar continually as they travel will be uniform in the direction of travel (or the "*x*" direction), and vary by distance from the ship track in the direction perpendicular to the direction of travel (or the "*y*" direction).

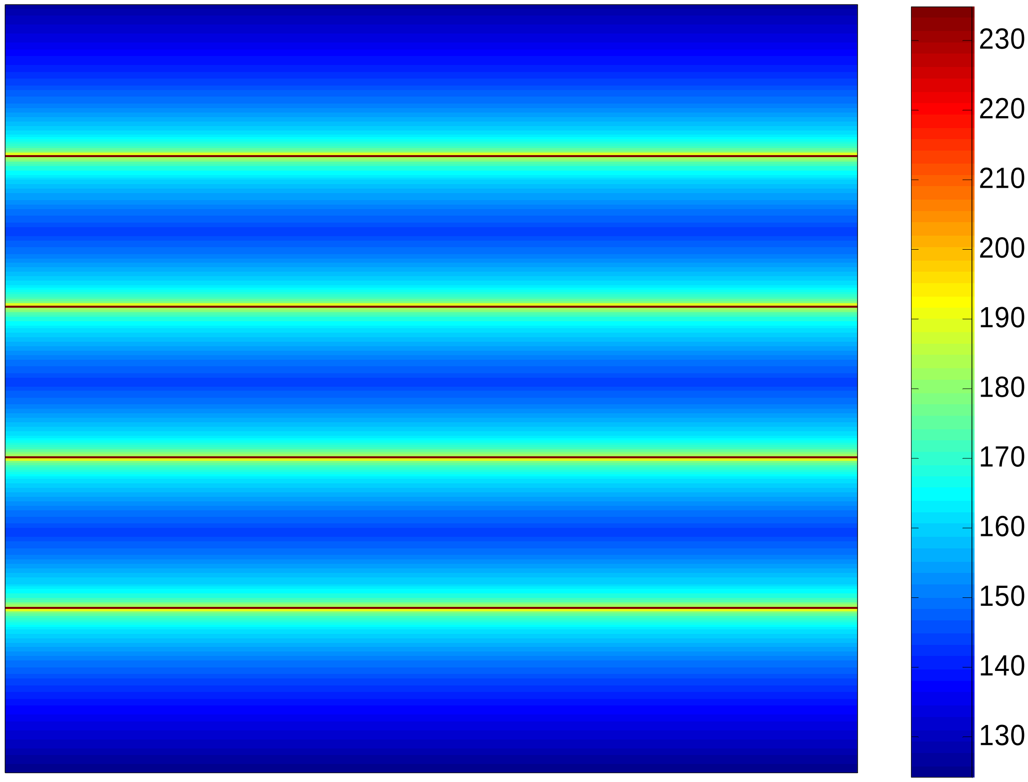

Figure D-32. – Sound Field Produced by Multiple Ships

This sound field of the four ships operating together (Figure D-32) ensonifies less area than four ships operating individually. However, because at the time of modeling, even the average number of ships and mean distances between them were unknown, a post-calculation correction should be applied.

As shown on Figure D-32, the sound field around the ship tracks, the portion above the upper-most ship track, and the portion below the lower-most ship track sum to produce exactly the sound field as an individual ship (Figure D-33).

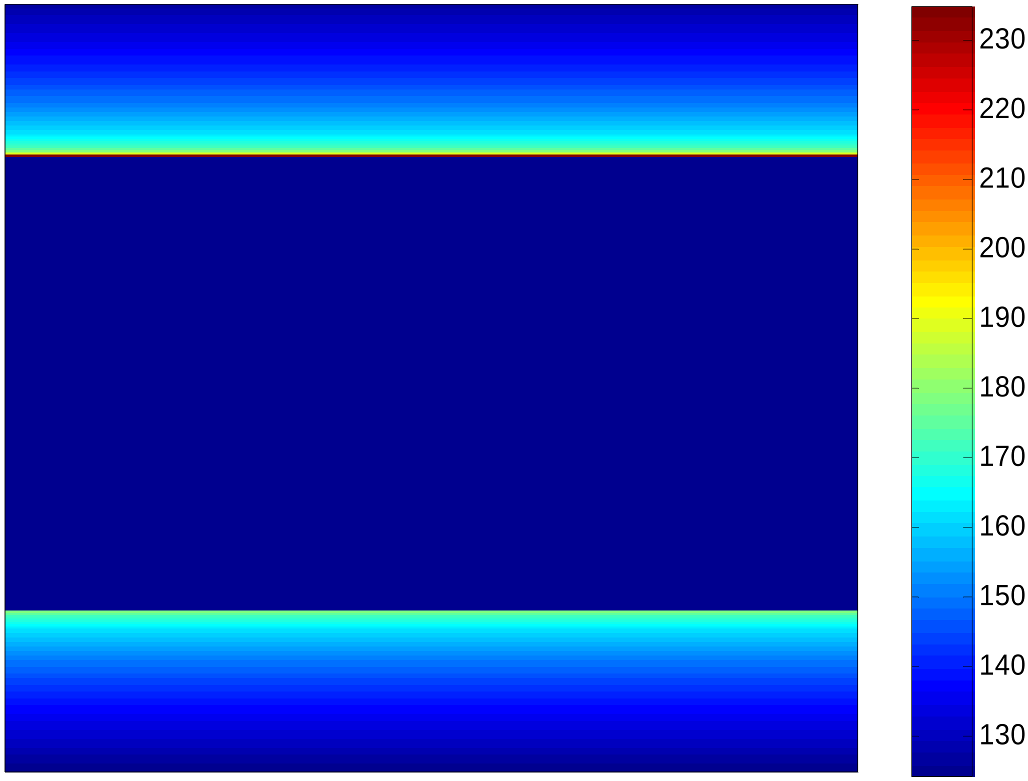

Figure D-33. – Upper and Lower Portion of Sound Field

Therefore, the remaining portion of the sound field, between the uppermost ship track and the lowermost ship track, is the contribution of the three additional ships (Figure D-34).

This remaining sound field is made up of three bands. Each of the three additional ships contributes one band to the sound field. Each band is somewhat less than the contribution of the individual ship because its sound is overcome by the nearer source at the center of the band. Since each ship maintains 20 km distance between it and the next, the height of these bands is 20 km, and the sound from each side projects 10 km before it is overcome by the source on the other side of the band. Thus, the contribution to a sound field for an additional ship is identical to that produced by an individual ship whose sound path is obstructed at 10 km. The work in the previous discussion on land shadow provides a calculation of effect reduction for obstructed sound at each range. An SQS-53-transmitting ship with obstructed signal at 10 kilometers across both seasons causes an average of 95% of the number of harassments as a ship with an unobstructed signal. Therefore, each additional ship causes 0.95 times the harassments of the individual ship. Applying this single-ship factor to the exercise type described earlier (three ships), the adjustment factor given this formation is approximately 2.90.

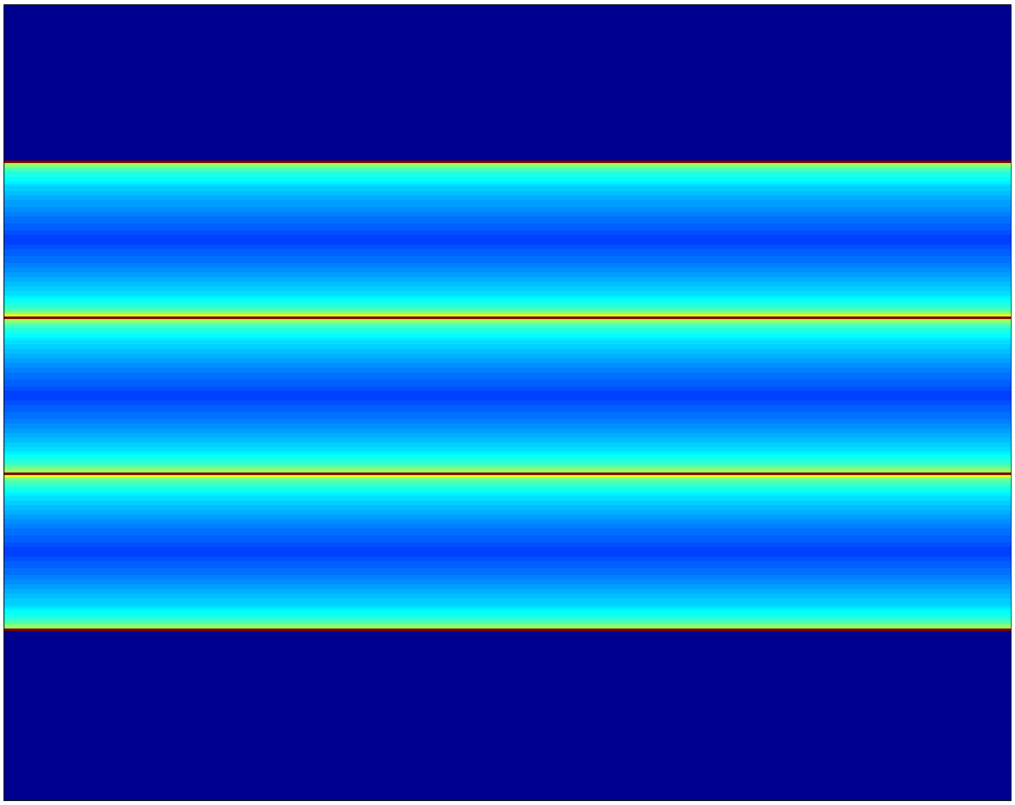

Figure D-34.– Central Portion of Sound Field

D.7 REFERENCES

Arons, A.B. (1954). "Underwater Explosion Shock Wave Parameters at Large Distances from the Charge," J. Acoust. Soc. Am. 26, 343.

Bartberger, C.L. (1965). "Lecture Notes on Underwater Acoustics," NADC Report NADC=WR-6509, Naval Air Development Center Technical Report, Johnsville, PA, 17 May (AD 468 869) (UNCLASSIFIED).

Christian, E.A. and J.B. Gaspin, (1974). Swimmer Safe Standoffs from Underwater Explosions," NSAP Project PHP-11-73, Naval Ordnance Laboratory, Report NOLX-89, 1 July (UNCLASSIFIED).

Department of the Navy (1998), "Final Environmental Impact Statement, Shock Testing the SEAWOLF Submarine," U.S. Department of the Navy, Southern Division, Naval Facilities Engineering Command, North Charleston, SC, 637 p.

Department of the Navy (2001), "Final Environmental Impact Statement, Shock Trial of the WINSTON S. CHURCHILL (DDG 81)," U.S. Department of the Navy, NAVSEA, 597 p.

Finneran, J.J., R. Dear, D.A. Carder, and S.H. Ridgway. 2002. Temporary shift in masked hearing thresholds in odontocetes after exposure to single underwater impulses from a seismic watergun. Journal of the Acoustical Society of America. 111:2929-2940.

Finneran, J.J., and C.E. Schlundt. 2004. Effects of intense pure tones on the behavior of trained odontocetes. Space and Naval Warfare Systems Center, San Diego, Technical Document. September.

Finneran, J.J., D.A. Carder, C.E. Schlundt and S.H. Ridgway. 2005. Temporary threshold shift in bottlenose dolphins (*Tursiops truncatus*) exposed to mid-frequency tones. Journal of Acoustical Society of America. 118:2696-2705.

Goertner, J.F. (1982), "Prediction of Underwater Explosion Safe Ranges for Sea Mammals," NSWC TR 82-188, Naval Surface Weapons Center, Dahlgren, VA.

Keenan, R.E., Denise Brown, Emily McCarthy, Henry Weinberg, and Frank Aidala (2000). "Software Design Description for the Comprehensive Acoustic System Simulation (CASS Version 3.0) with the Gaussian Ray Bundle Model (GRAB Version 2.0)", NUWC-NPT Technical Document 11,231, Naval Undersea Warfare Center Division, Newport, RI, 1 June (UNCLASSIFIED).

Ketten, D.R. 1998. Marine mammal auditory systems: A summary of audiometric and anatomical data and its implications for underwater acoustic impacts. NOAA-TM-NMFS-SWFSC-256, Department of Commerce.

Kryter, K.D., W.D. Ward, J.D. Miller, and D.H. Eldredge. 1966. Hazardous exposure to intermittent and steady-state noise. Journal of the Acoustical Society of America. 48:513-523.

McGrath, J.R. (1971). "Scaling Laws for Underwater Exploding Wires," J. Acoust. Soc. Am. 50, 1030-1033 (UNCLASSIFIED).

Miller, J.D. 1974. Effects of noise on people. Journal of the Acoustical Society of America. 56:729–764.

Nachtigall, P.E., J.L. Pawloski, and W.W.L. Au. 2003. Temporary threshold shift and recovery following noise exposure in the Atlantic bottlenose dolphin (*Tursiops truncatus*). Journal of the Acoustical Society of America. 113:3425-3429.

National Oceanic and Atmospheric Administration (NOAA). 2001. Final Rule Taking and Importing Marine Mammals: Taking Marne Mammals Incidental to Naval Activities --The Shock Trial of the WINSTON S. CHURCHILL (DDG-81), Federal Register, Department of Commerce; NMFS, FR 66, No. 87, 22450-67.

National Oceanic and Atmospheric Administration, 2002. "Final Rule SURTASS LFA Sonar," *Federal Register*, Department of Commerce; NMFS, *Federal Register,* Vol 67, No. 136, pp. 46712-46789.

Schlundt, C.E., J.J. Finneran, D.A. Carder, and S.H. Ridgway. 2000. Temporary shift in masked hearing thresholds of bottlenose dolphins, *Tursiops truncatus*, and white whales, *Delphinapterous leucas*, after exposure to intense tones. Journal of the Acoustical Society of America. 107:3496-3508.

Urick, R.J. (1983). Principles of Underwater Sound for Engineers, McGraw-Hill, NY (first edition: 1967, second edition: 1975, third edition: 1983) (UNCLASSIFIED).

Ward, W.D. 1997. Effects of high-intensity sound. In Encyclopedia of Acoustics, ed. M.J. Crocker, 1497-1507. New York: Wiley.

Weston, D.E. (1960). "Underwater Explosions as Acoustic Sources," Proc. Phys. Soc. 76, 233 (UNCLASSIFIED).

Yelverton, J.T., D.R. Richmond, E.R. Fletcher, and R.K. Jones, 1973. "Safe Distance from Underwater Explosive for Mammals and Birds", Technical Progress Report, DNA 3114T, Department of Defense, Defense Nuclear Agency, Washington, D.C., April.

Yelverton, J.T. 1981, Underwater Explosion Damage Risk Criteria for Fish, Birds, and Mammals, Manuscript, presented at 102nd Meeting of the Acoustical Society of America, Miami Beach, FL, December, 1982. 32pp.